# POWER SPECTRAL ANALYSIS OF SURFACE MYOELECTRIC SIGNALS DURING DYNAMIC CONTRACTIONS

A Thesis

Submitted to the College of Graduate Studies and Research

in Partial Fulfillment of the Requirements

for the Degree of

Master of Science

in the

Division of Biomedical Engineering

University of Saskatchewan

by

SHANKAR SRINIVASAN

Saskatoon, Saskatchewan

March 1988

UNIVERSITY OF SASKATCHEWAN

DEPARTMENT OF BIOMEDICAL ENGINEERING

## CERTIFICATION OF THESIS WORK

We, the undersigned, certify that Srinivasan SHANKAR, candidate for the Degree of Master of Science in Biomedical Engineering, has presented his thesis on the subject Power Spectral Analysis of Myoelectric Signals

that this thesis is acceptable in form and content, and that this student demonstrated a satisfactory knowledge of the field covered by his thesis in an oral examination held on March 22, 1988.

External Examiner: Brian R McIntosh

of PHYSIOLOGY

Internal Examiners:

Bruce R. Brandell

[illegible]

[illegible]

Robert [illegible]

[illegible]

Date: March 22, 1988

# COPYRIGHT

# ACKNOWLEDGMENTS

The author would like to express his gratitude and appreciation to Dr. Robert E.Gander for his guidance and consistent encouragement throughout the course of this work. His advice and assistance in the preparation of this thesis is thankfully acknowledged. The author would also like to thank Dr. Bruce R.Brandell for his timely and beneficial suggestions and also help in the preparation of this thesis.

The author takes this opportunity to acknowledge the encouragement and moral support provided by his Mother and all other family members.

Financial assistance provided by the University of Saskatchewan in the form of Graduate Scholarship is thankfully acknowledged.

This work and the thesis would not have come about but for the volunteering of eleven 'brave' colleagues, namely, A.J.P, A.B, B.N, B.P, D.W, E.P, M.P, M.N, R.T, H.K.S, and U.B. May their tribe increase!

UNIVERSITY OF SASKATCHEWAN

Biomedical Engineering Abstract 88A285

# POWER SPECTRAL ANALYSIS OF SURFACE MYOELECTRIC SIGNALS DURING DYNAMIC CONTRACTIONS

Student: Shankar S Supervisors: Dr. R.E. Gander
Dr. B.R. Brandell

M. Sc. Thesis Presented to the

College of Graduate Studies and Research

March 1988

## ABSTRACT

The stochastic nature of surface myoelectric signals (MES) requires the use of power spectral analysis for effective characterisation. Spectral changes during different types of muscular activity are monitored using spectral parameters like mean power frequency, ratios of powers in several arbitrarily chosen spectral bands and median frequency. The median frequency has been shown to be a reliable indicator of such changes during static contractions. Few such studies, however, are available in the literature for dynamic contractions.

In this work, non-fatiguing, isotonic, constant velocity contractions of the right biceps brachii m. were studied. The median frequency and the spectral power were chosen as test indicators of any changes that may occur due either to the loading of the muscle, the angular velocity of contraction or the changes in joint angle (and hence the muscle length).

A significant increase in median frequency was found with the loading of the muscle and also for a decrease in joint angle. On the other hand, no variation was observed due to velocity changes. The spectral power confirmed the expected dependence with loading, angular velocity of contraction and joint angle.

# Table of Contents

# List of Figures

# List of Tables

# Chapter 1
# MUSCLE AND MYOELECTRIC SIGNALS

## 1.1. Introduction

Inherent movement is a prime sign of the existence of life. For this and many other reasons, man has studied locomotion of his own and of other creatures and continues to do so even today.

When Galvani's experiments brought to light the electrical aspect of muscle movement, a new dimension was added to the study. Further discoveries connecting electricity and muscle contraction caused the study to be an area of its own importance and thus, the field of electromyography was born.

For detecting the electrical signal which emanated from the muscle upon its contraction, two kinds of electrodes came into being. The surface or skin electrodes to be used on the skin surrounding the muscle and the needle electrode which was inserted into the muscle.

In the early part of this century, Hill, Sherrington and others using both kinds of electrodes conducted a large number of experiments, and with the results that followed, they formulated simple but elegant theories concerning muscular activity. Electromyography became a quantitative discipline encompassing not only electrical and mechanical but also, thermal and chemical studies. Subsequent theories and experimental techniques derived from mechanics, biochemistry, microscopy, molecular biology, electronics and thermodynamics, have yielded a great amount of information about the structure and function of the muscle and the myoelectric signal acquired from it. A synopsis of the above stated information gleaned from perusing the relevant literature is presented in the following sections.

## 1.2. Motor Units and Motor Unit Action Potentials

The muscle tissue is specifically differentiated from the other tissues in the mammalian body for the purpose of contraction and in the process effecting motion either in an organ (smooth and cardiac muscle types) or upon the skeletal framework of the body (skeletal muscles). In this study, only the latter muscle type will be referred to since it is of direct relevance to it.

In normal skeletal muscle, its structural units - the muscle cells or fibres - never contract individually. Instead small groups of them contract almost simultaneously, the reason being they are innervated by individual nerves, each nerve associated with a group ranging from 7 to 1200 muscle fibers. The variation in the size of these groups called *motor units*, is due to the variable sensitivity required of a movement associated with a contraction. Again, biochemically, muscle fibres have been differentiated into Slow Twitch and Fast Twitch fibres based upon their contracting response to a nerve impulse descending down the axon from a nerve cell of the central nervous system. Thus, a single muscle equipped with both kinds of fibres (slow and fast) and an admixture of different sized motor units all in a proportion dependent upon the role of the muscle is a very flexible and efficient biological machine.

The electrical activity associated with a motor unit is the summated response of the individual muscle cells and is called a *motor unit action potential* (MUAP). During a muscle contraction, the motor units are fired repetitively, and the resulting discharge of MUAPs is called a *motor unit action potential train* (MUAPT). Also, for a given muscular contraction several motor units become active, the number of them and the rates at which they 'fire' differ, depending upon the load put upon the muscle. Indeed, the increase in the number of active motor units is called 'Recruitment' while, the variation of the firing rate to accomodate the given load upon the muscle, is called 'Rate Coding'. Hence, a detecting electrode will detect a summated response of MUAPTs each with its own 'firing rate' and this response is called a myoelectric signal (MES). Both the firing rate and the recruitment processes being random in nature, therefore, the myoelectric signal ensues to be a stochastic process. To illustrate the above, use is made of a simple model proposed by De Luca [11] and which is schematically illustrated in Figure 1-1.

The MES is synthesised by linearly summing the MUAPTs as they exist when they are detected by the electrode. In the figure, the integer $p$ represents the total number of MUAPTs which contribute to the potential field at the recording site. Each of the MUAPTs are modelled by considering them to be the output of a transfer function $h(t)$ with a model of a MUAP (in this case, that proposed by De Luca), with the input being Dirac delta impulse trains

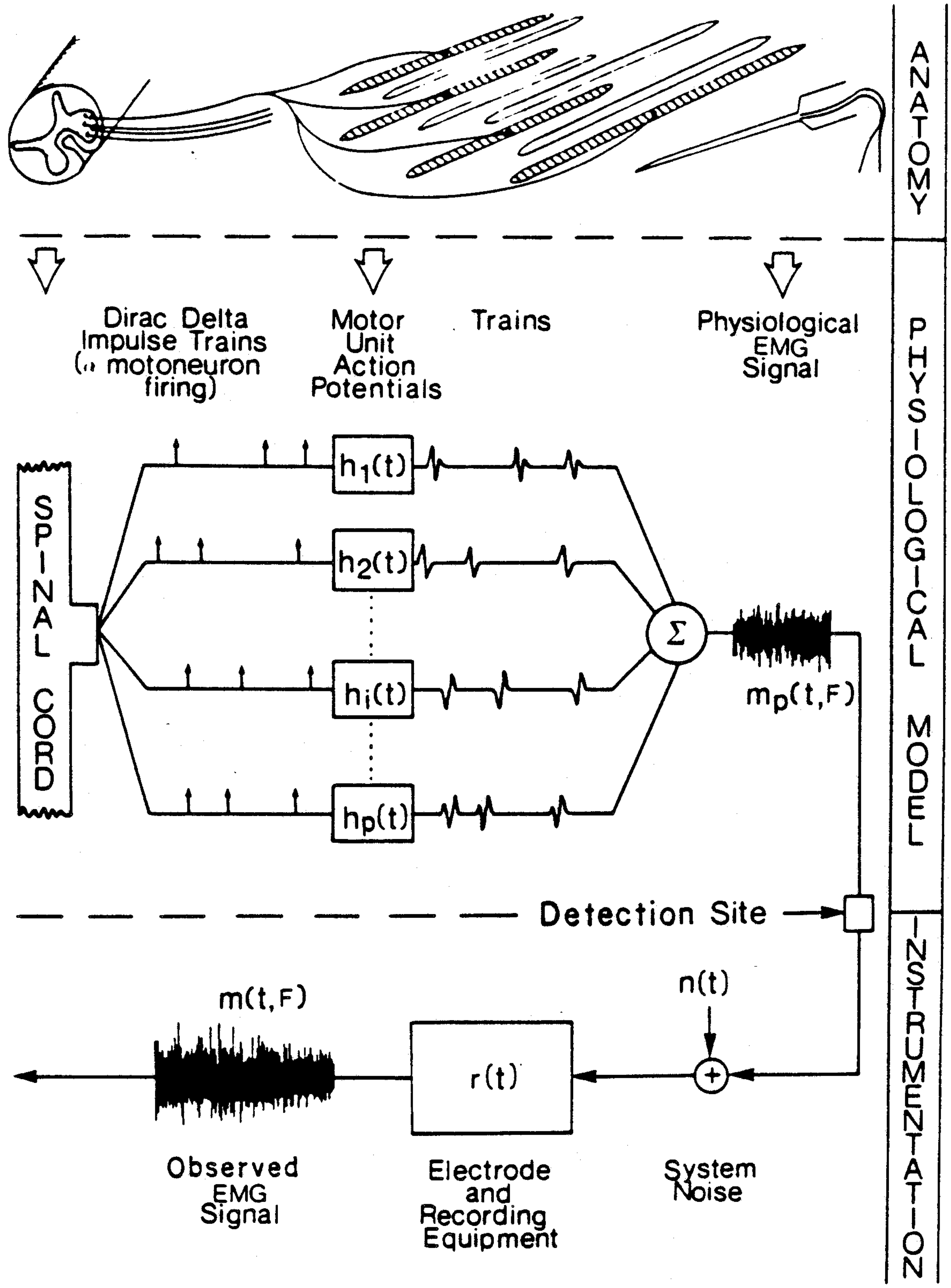


**Figure 1-1**: Schematic Illustration of the Physiological and Electrical Correlates of the Myoelectric Signal

representing the nerve axonal impulses travelling down from the motoneurons. The observed MES could be that using a needle electrode or a surface electrode. The noise introduced during detection and the filtering properties of the electrode set-up, and possibly other instrumentation are shown as time dependent functions n(t) and r(t). The real MES $m_p(t,F)$ and the observed signal m(t,F) both have time dependence as well as force dependence too [11]. Though the indwelling needle electrodes could detect the individual MUAPTs upon weak muscle contractions, it is an invasive method of obtaining information. A non-invasive method such as surface electrodes is therefore preferable and is the one used in this study.

During the 1960s, the widespread use of computers in communication systems analysis and signal processing brought into light the advantages of using what was called 'power spectral analysis', related very much to Fourier analysis which has been widely studied for over two centuries. The enormous amount of calculations required for computing signal spectra had deterred researchers from approaching it as a means for obtaining information from random signals. Thus the development of low cost, faster computers and computing techniques for signal processing helped bring about such a move, and very soon, spectral analysis became a widely used and researched tool for the analysis of myoelectric signals as well.

## 1.3. Objectives of the Study

In this study, power spectral analysis was decided to be used in analysing non-fatiguing isotonic contractions of the right biceps brachii m. The factors studied in relation to this were the Applied Torque, the Angular Velocity of Contraction and the Muscle Length itself (in terms of the Joint Angle, which is the angle between the upper arm and the forearm), since it undergoes changes during the contraction. Two parameters associated with a power spectrum, namely, the Median Frequency and the Total Spectral Power, were used as indicators for any spectral changes that may occur due to either or all of the above factors. To the knowledge of the author, no complete study has been made so far along the lines described. The prime purpose of this study was intended to get a better understanding of the relationships that may exist between the underlying physiological processes and the emanated myoelectric signal. Also, it could have potential clinical application in diagnosing muscular dysfunction. Another significant application could be found in the fact that noise-immune frequency-control methods are sought for in the presently amplitude-controlled prosthetic devices. In this context, the median frequency and/or the spectral power could be used as control parameters individually or augmenting the present mode of amplitude control.

## 1.4. Outline of the Thesis

With the objectives of the study as stated above, chapter 2 is therefore, devoted to explaining spectral analysis and its usefulness in the analysis of myoelectic signals, compared to amplitude analysis methods used so far.

The experimental aspects of this study viz., the apparatus used, the analytical tools employed and the experimental procedure itself, are detailed in Chapter 3. Reasons for choosing the said factors and spectral parameters are also put forth.

Chapter 4 shows the results of all the analyses. These include the power spectral analyses and several statistical analyses involved in getting a clearer picture of the results obtained.

The discussion of the results of the analyses is dealt with in Chapter 5. Correlating the obtained results with those available from related work is also done.

Chapter 6 carries the conclusions of the work detailed in this thesis. A few speculations as to the important results of the work are put forth.

Appendices A and B detail the mathematical aspects of power spectral analysis and the specific computer procedures employed to do the same. Appendix C carries the raw tabulated data as obtained in the several experiments conducted in this work.

# Chapter 2
# SPECTRAL ANALYSIS

## 2.1. Introduction

The power spectrum is perhaps the single most descriptive characteristic of a random process of which the myoelectric signal is a typical example. Power spectral estimation or analysis of MES has had a growing importance during the past two decades, since it proved to be a method of obtaining more information from this noise-like signal than time domain analysis could provide.

Spectral analysis can be better understood to be the decomposition of a signal into sinusoids of different frequencies or into travelling waves of different length in the case of propogating action potentials. The strength of these components or potentials as a function of the frequency is called the spectrum of the signal. The strength may be in terms of amplitude which would be to the same scale as of the signal or it may be in terms of power, which is on a amplitude-squared scale. The latter is specifically called the power spectrum and being of more relevance to this study, it would henceforth be used synonymously with the term 'spectrum' or 'spectral analysis'.

There are two important aspects to the technique of spectral analysis. One is that it is a means of detecting hidden periodicities in the signal, be it deterministic or probabilistic. The other aspect is its ability to characterise random signals which in the time domain, could only be characterised in probability terms. That is, a probability distribution is all that could characterise the signal and this was not sufficiently informative. The power spectrum is thus an important source of information applicable to a variety of signals: random as well as deterministic, either periodic or aperiodic ones.

## 2.2. Time Domain Analysis of MES

If a physical phenomenon of interest is random, then each time history record $x(t)$ of that phenomenon represents a unique set of circumstances which is not likely to be repeated in other independent measurements of that same phenomenon. Hence, to completely define all properties of the phenomenon, it is necessary to conceptually think in terms of all the time history measurements $\{x(t)\}$ that might have been made. In general, an infinite number of such conceptual measurements is required to fully describe the phenomenon. It follows that the instantaneous amplitude of the phenomenon at a specific time $t_1$ in the future or from a different experiment has to be defined in probabilistic terms. Two probability measures used to do so are the Probability Distribution Function and the Probability Density Function. The probability distribution function $P(x)$ is defined as the probability of the event that the observed random variable, say 'X', is less than or equal to an allowed value 'x'. That is, $P(x)=Prob[X \leq x]$. Although the distribution function is a complete description of the probability model for a single random variable, it is not the most convenient form for many calculations of interest. For such cases, the probability density function $p(x)$, which is the derivative of the probability distribution function $p(x)=d/dx[P(x)]$ is used. For non-stationary random processes, both the functions vary as time $t_1$ varies. On the other hand, both remain constant, with time, for stationary processes. The relevance of these two functions lies in the fact that random data can be effectively characterised by using them. That is, the central tendency (Mean) and the dispersion (Variance), gathered from the probability distribution and the density functions characterise the random process in the time domain. Indeed, time domain analysis of MES has been widely done and some of the results so obtained are reviewed below.

Milner-Brown et al. [33] using the average rectified value of the surface MES in isometric contractions, found that a linear relationship existed between it and and the force applied. Hagberg et al. [14] using the rectified and filtered MES found a correspondingly linear relationship between the force and the amplitude during both isometric and isotonic contractions.

Integration of the MES has been the most widely studied and abused procedure [1]. The output from a linear envelope detector following rectification of the MES had been wrongly considered as an integration operation and the output was termed as 'IEMG' (Integrated ElectroMyoGram). Reasons quoted by De Luca [1] as to such a usage are its historic precedence and also the observation that for a sufficiently long integration time, the integrated rectified value of the MES provides a smoothly varying measure of the signal as a function of time.

Bigland et al. [4] had stated that a linear relationship existed between the integrated MES amplitude and force in different types of contractions. This has been confirmed by Komi [20], Bouisset et al. [6], Moritani [35] and others.

Other mechanical parameters such as velocity of contraction, acceleration and work output have also been studied but not so widely as for force as listed above. For example, Bigland and Lippold [4] showed that the IEMG bore a direct linear relationship to the angular velocity of movement under conditions of constant load. Komi [20] and Danoff [10] also found similar relationships. Studying the triceps, Scherrer et al. [41], found a linear correlation between IEMG and mechanical work. Patla et al. [38] developed a model relating a muscle's mechanical output to the MES upon the basic assumption that a constant quantum of energy (chemical) is released per MU firing. They suggest, on the basis of their model being successful in corroborating the experimental results obtained from literature, that the MES is directly related to the muscle mechanical power via a non-linear differential equation in terms of the velocity of contraction.

Miwa and Matoba [34] found that the amplitude of the MES varied as the joint angle of the biceps brachii changed. At 160 deg joint angle, they observed maximum myoelectric activity while at 90 degrees it was almost 'nil'.

From the foregoing paragraphs, one may observe that quite a bit of information has been gleaned from the noise-like myoelectric signal. But there was always felt a need to obtain more information than could be gathered from its amplitude aspect alone. Power spectral analysis which had been effectively used in analysing random phenomena in engineering processes was therefore resorted to. An important advantage of using spectral analysis stems from the fact that a wide range of engineering applications of random data analysis centers around the determination of linear relationships between two or more sets of data. These linear relationships are possible to be extracted in terms of spectral density functions. For example, it is possible to correlate the spectra related to the input nerve impulse trains with that of the output MES using models such as the one detailed in the previous chapter. Thus, the usage of power spectral analysis is found favourable for a better understanding of the MES and its physiological counterparts.

## 2.3. Spectral Analysis of MES

Once the need for spectral analysis of MES was felt, there have been many rigorous methods, mathematical and physical, developed for the analysis and several experiments have been conducted to formulate and prove some of the important mathematico-physical models of the MES and its underlying physiological processes. From these researches, much knowledge has been gained which has since then been confirmed. A review of the literature for some of the important observations made regarding the MES and its related power spectra follows in the forthcoming paragraphs.

To study or monitor the spectral changes, however, requires some parameters or measures for detecting and to quantify them. Some of the well-defined measures are the mean power frequency, median frequency, bandwidth, spectral power or energy, and peak power frequency. These terms are defined in appendix A. Using one or more of these parameters, the following observations have been made about the MES.

McLeod et al. [31] noted that the power spectra of the MES detected from intramuscular electrodes generally has a bandwidth ranging from 0 to 1 kHz while using surface electrodes the bandwidth was just 0 to 500 Hz.

Zipp [44] studying different electrode configurations (such as monopolar or bipolar), noted that the inter-electrode spacing in bipolar configuration is inversely proportional to the spectral bandwidth. Shifting of the electrodes around the circumference of the limb however, did not alter the bandwidth.

Lindstrom [30] using computer simulated action potentials noted that the envelope of the spectrum corresponding to a single MUAP was preserved with a spectrum corresponding to a summation of randomly selected MUAPs.

Le Fever and De Luca [27], studying the contribution of individual MUs to the ME power spectra, showed that, in the frequency range of DC to 40 Hz, the power spectrum of the individual MUAPT is affected primarily by the interpulse intervals (IPI) statistics. A significant peak was observed at a frequency corresponding to the firing rate and progressively lesser peaks at harmonics of the firing rate. Beyond 40 Hz, they observed that the power spectrum is essentially determined by the shape of the MUAP.

A similar observation was made by Lago and Jones [25] who suggested that from the analysis of the low frequency region of the MES spectrum it is possible to extract some information on the MU firing properties. This information, they said was the average discharge rate of the population of active units, and the dispersion of those discharge rates.

In confirmation with both of the above, Boxtel and Schomaker [7] upon studying non-fatiguing, sub-maximal, static contractions of the facial muscles, noticed a distinct peak in the power spectral region below 40 Hz. They showed it to be a genuine MES activity and not a motion artifact. An increase of contraction strength resulted in a shift of the peak to higher frequencies and a decrease in its amplitude relative to the estimates above 40 Hz. According to their mathematical model, this peak indicates the dominant firing rate of the sampled MUs and which is that of the first recruited low-threshold MUs. Differences in firing rate statistics, they speculate, might cause its non-appearance in the spectra of larger muscles such as those of the limbs.

Sato [40] having studied the surface MES of different muscles, observed that, the spectral patterns differ from one muscle to another. For example, the upper limb muscles displayed a narrower bandwidth (0 to 160 Hz) compared to those from the lower limb and abdominal muscles (0 to >300 Hz). He discounts the hypothesis that differences in MU activities, such as variations in amplitude, duration, and discharge rate, explain the different MES spectra in different muscles systematically. He suggests that many more studies are required to look into the factors affecting the MES power spectra before any firm conclusions could be drawn. He also studied the effect of right or left-handedness and found no variation in the power spectra.

Lindstrom et al. [29] attempted an interpretation of the MES power spectrum based on a mathematical model and then analysed different parameters which influence the spectrum. Some of the observations they put forth are:

- there exists a distance-dependent, low-pass filtering effect of the tissue intervening between the electrodes and the active MUs. For example, a distance of only a millimeter from an active fiber causes an attenuation of frequencies greater than 1.5 kHz by nearly 30 dB.

- MU size cause differences in the low and high frequency content of the spectra. Small muscles, which generally have fewer fibers per MU, will show power spectra containing relatively higher amount of high frequency activity than will muscles with larger MUs. This is because, as a greater number of MUs combine, the greater is the chance of high frequency waves cancelling one another while the low frequency waves summate. An estimate of the number of MU fibres could thus be formed by observing the MUAP's power spectrum.

- the bipolar electrode configuration (when lined along the direction of the fibres) introduced so-called 'dips' in the power spectrum at those frequencies which correspond to the inter-electrode distance being a multiple of the wavelengths. The positions of these dips are uniquely determined by the electrode size and the propogation velocity of the MUAPs. Therefore, they proved to be an effective means of computing the conduction velocity in the MU fibres. The conduction velocity, as one may note from the forthcoming observations is closely associated with the muscle's internal conditions such as its temperature, acidic level, and state of fatigue.

The effectiveness of the use of MES in the assessment of neuromuscular disorders has often been investigated. Frequency analysis has yielded consistent observations regarding spectral changes in both neuropathy and myopathy. Larsson [26] studied neuropathies induced by lesions of the peripheral motor neurons. His results suggested that the spectrum shifted to lower frequencies in neuropathies with a clinical history of at least 6 months. This was consistent with the observation made of the MUAPs to have longer time durations in such cases. He suggests that, since a characteristic frequency (median frequency, for example) is sensitive to the 'average' shape of the MUAPs, therefore, it could be useful in following the development of the disorder. In the case of myopathy, an opposite effect on the shape of the MUAPs was noted by Kugelberg [22] who found that they are generally shorter in duration and more often polyphasic. This result was confirmed in the frequency domain by Kopec and Hausman [21] who noted that the spectra shifted to higher frequencies in such cases.

Environmental factors (internal and external) such as temperature, ischemia, and blood lactate levels have also been observed to cause significant spectral changes. For example, Merletti et al. [32] showed that the median frequency decreased upon occlusion by external compression of the blood vessel in the contracting muscle. Their results are consistent with the fact, they state, that when the blood is occluded, acidic by-products accumulate in the environment of the muscle fiber membrane and they decrease the conduction velocity of the fiber. Also, an increase in muscle temperature from $10^0$ to $40^0$C was found to cause an increase in the median frequency by Petrofsky and

Lind [39]. Merletti et al. [32] found the median frequency to decrease linearly with decreasing muscle temperature. Both groups attribute the cause to the conduction velocity being directly related to muscle temperature.

An important and most studied muscle characteristic is fatigue. Since the concept of fatigue is a very broad one and hence ambiguous if stated just as fatigue, there has been developed a specific term *localised muscular fatigue* relevant to the study of the MES. This term refers to that state of the muscle which is induced by a sustained muscular contraction and which is associated with external manifestations such as the inability to maintain a desired force output, muscular tremor and localised pain [1].

In the study of localised fatigue, it has been predominantly observed that the power spectrum shifts significantly towards the lower frequencies in a variety of muscles throughout the human body. For example, Kadefors et al. [18] found that the low frequency components of the ME power spectra, in the biceps brachii, increased while the higher frequency components decreased as fatigue developed. At the same time there was noted a significant increase in the MES amplitude. Lindstrom et al. [28] and Kwatny et al. [24] among a host of others, have noted similar changes. It has been consistently observed that the spectral shift to the lower frequencies is due to a decrease in muscle fiber conduction velocity which in turn was caused by an accumulation of acidic by-products. Motor unit synchronization and recruitment of larger MUs along with a decrease in conduction velocity as fatigue developed have been noted as significant factors in the amplitude increase and the spectral shift by Naeiji and Zorn [37].

During a sustained muscular contraction, both the mean and the median frequencies were noted to decrease as a function of time. More than 50% decrease in value from the beginning to the end of the sustained contraction has been noted at around 50% MVC by Clamann and Broecker [9] and was confirmed by Tesch and Karlson [42] who found that maximal lactate concentration was found in muscles which contracted isometrically at 50% MVC to exhaustion. This phenomenon has again been attributed by all of these researchers as due to a decrease in conduction velocity. Indeed the currently known factors that determine directly or influence the waveform of the MUAPs and hence the power spectrum are outlined below:

1. Tissue filtering caused by differences in muscle fiber and electrode locations.

2. Conduction velocity of muscle fibers which is monotonically related to the fiber diameter and is greatly affected by the intramuscular pH. The latter is dependent upon the functional capacity of the vascularization in the muscle and the force level of contraction.

Apart from the study of the basic characteristics of the ME power spectrum briefed above, the relations that exist between the strength of muscular activity and the associated myoelectric power spectra have also been looked into. There have been various studies concerning force or tension upon the muscle. These concern static muscular contractions at both low levels and high levels of tension.

Hagberg and Ericson [15] studied the isometric contractions at 5-80% MVC of the biceps brachii, brachialis and brachioradialis. They found that the mean power frequency increased with contraction level up to 30% MVC and then flattened out, for all the three muscles. They attribute the observed shift at low levels to tissue filtering effect. That is, as contraction level increased, large MUs closer to the surface are recruited, the electric potential from these muscle fibers suffer less high frequency attenuation through the overlying tissue and thus the power spectrum shifts to higher frequencies. The flatter aspect of the relationship is, they state, possibly caused by fatigue due to insufficient rests given to the subjects.

Gander and Hudgins [12] studying non-fatiguing static contractions of the biceps brachii confirmed those results. They also show that a peak appearing in the low frequency region (below 40 Hz) shifted to higher frequencies with an increase in load. They have noted, therefore, that a combination of recruitment and rate coding is responsible for the increase in median frequency. Their observations are consistent with those of Gydikov and Kosarov [13] and Blinowska et al. [5].

However, Sato [40] studying the effect of contraction level on the MES and its power spectra found no systematic variation in their pattern.

Consistent observations have been made by both Inbar et al. [17] and Bazzy et al. [2], concerning muscle length changes causing shifts in the spectrum towards the higher frequencies. The former group computed the median frequencies at three joint angles (45,90 and 135 degrees) of the biceps brachii and extensor digitorum and they found it to decrease with the increase in joint angle (and correspondingly the muscle length). They reason that the change in muscle shape with flexion of the biceps may cause the shift while it was less likely in the extensor digitorum. Bazzy et al., also, studied the relationship between changing elbow angle and the ME power spectra of the biceps brachii, during sub-maximal non-fatiguing isometric contractions. Two joint angles (45 and 135 degrees) were held against a constant load of 3 kgs. They found a decrease in mean power frequency with the increase in joint angle. A change in the electrode position relative to the underlying muscle or the activated motor units was stated to be a cause for such an effect.

Myoelectric activity during dynamic contractions of a muscle has been studied almost exclusively in the time domain. A briefing about some of the results pertaining to the same was done in the previous section. However, in the frequency domain, very little work has dwelled upon this important area. Muro et al. [36] studying non-fatiguing isotonic contractions at different loads ranging from 0.25 to 3.0 kgs, at an angular velocity of $90^0$ per second, observed that the mean power frequency progressively increased (total increase around 8 Hz) with load. Actually, they conducted the experiments with different groups (healthy, neurogenic and myogenic) to obtain clinically useful information regarding neuromuscular changes affecting the surface MES and its power spectrum. Besides this work, there has been no other, to the author's knowledge, in the literature, pertaining to power spectral analysis of dynamic contractions.

## 2.4. Summary

In the field of engineering, power spectral analysis has been effectively used to characterise random signals. Therefore, analysis of the power spectra of the myoelectric signal may be a reasonable starting point for an exploration of its properties as well. Indeed, much information is currently available relating spectral parameters to changes in the muscle's internal and external environments. Muscle pathology has been studied with reference to differences between normal and pathology related MES spectra. As regards muscular activity, static contractions have been widely studied and many observations have been repeatedly confirmed. But, the dynamic contraction of a muscle has not been equally well studied. Much remains to be known in relating muscle movement to spectral changes. Hence, as stated in the previous chapter, the study relating to this thesis was undertaken to try fill up the "gap". In the next chapter, the experimental aspects of the study as regards the apparatuses used, the experimental methodology and the processing of the data are discussed in detail.

# Chapter 3

# MATERIALS AND METHODS

## 3.1. Selection of Muscle

Amongst the several muscles of the human body, the biceps brachii is the most studied with reference to kinesiological studies. Much information of more or less *a priori* character is available about the muscle as regards its anatomical and physiological aspects. Also, it is one of the few easily accessible muscles for use with surface electrodes. As such, it was chosen as the test muscle for this study as well.

## 3.2. Choice of Spectral Parameters

As was mentioned in the previous chapter, there have been a few very widely used spectral parameters for monitoring spectral changes such as the mean power frequency, median frequency, peak power frequency and ratios of powers in spectral bands. Amongst these the peak power frequency is the least reliable since it is highly susceptible to statistical variations in power spectral estimation. The ratio parameter is again a matter of choice since the spectral bands are arbitrarily chosen, and it would be difficult to make any objective comparisons with other studies in the literature. However, looking at the power spectrum one can note that there can be two variations possible. There could be a shift in the spectrum either towards the lower frequencies or to the higher frequencies or there could occur an overall magnitude increase or decrease. Thus, either the mean power frequency or the median frequency would serve to monitor the first case; while the spectral power (equal to the area beneath the power spectral curve) is the ideal parameter for the second and hence was readily chosen. The median frequency was chosen over the mean power frequency because of its being relatively less sensitive to noise than the mean frequency, its ease of computation and moreover, it has been shown by Inbar et al. [17] that the two are related to each other through a constant multiplier.

## 3.3. Experimental Protocol

The experimental protocol of this work consisted of two studies. The first study dealt with spectral analysis of signals obtained during non-fatiguing static contractions at different joint angles. Two loads were used so as to serve two purposes. Firstly, it could enable confirmation of results available in literature of the median frequency varying at any joint angle with a change in loading. Secondly, any changes in the median frequency and/or spectral power with changes in joint angle itself could be noted and thence confirmed using two different loads.

The second study pertained to non-fatiguing, isotonic, constant velocity contractions. Changes in the applied torque or the angular velocity of contraction, causing any spectral changes which could be noted by the median frequency and/or the spectral power, were to be studied. The details of the protocol so defined are put forth in the subsequent sections.

## 3.4. Experimental Details

### 3.4.1. Apparatus Used

The skeleton at all its joints has lever arrangements with the muscles associated with those joints. During a voluntary contraction of a muscle acting across its associated joint, it is important to know not only the external force applied but also its point of application. That is, the applied torque has to be known. Since in this study various loads were to be moved at various velocities, the points of application of these loads must be the same for comparisons to be made. A distance of 250 mm distal to the elbow joint was found convenient and therefore was selected as the point of application of the four loads selected (see next section).

The applied torque, however, should be the same during the course of the forearm movement for comparison purposes again. This necessitates a wheel-like arrangement exerting a force at a fixed angle at the same point of application, throughout the course of the movement of the forearm, and with the elbow joint coinciding with the axis of the wheel. This indeed was the arrangement used in this study. After due considerations of the biomechanical aspects of the upper limb, a mechanical forearm loading apparatus, shown in the photograph in Figure 3-1 was designed and fabricated in the College of Engineering Workshop.

Supports shown at the wrist and at the upper arm levels prevent undesirable motion at either of them. The apparatus also had a provision for

**Figure 3-1:** The Forearm Loading Apparatus used for the experiments

coupling a potentiometer to the shaft of the wheel so as to monitor, with the help of an oscilloscope, the movement or the position of the wheel and hence of the forearm.

### 3.4.2. Test Parameters Used

For the first study, there were two loads to be held as mentioned earlier. In the first case a load of 19.6N was to be held at eight joint positions (165 to 60 degrees with intervals of 15 degrees). In the other, a load of 29.4N was to be held at three joint angles (150, 90 and 60 degs).

There were four loads to be associated with four different velocities for the second study. In all, therefore, sixteen test conditions were subjected upon each volunteer. The choice of the torques (1.23, 2.45, 3.68 and 7.35 Nm) and of the velocities (40, 80, 120, 160 deg/s) were based on the need for a sufficiently wide range of parameter values to be imposed and upon the comfort of the subject too. The latter refers to the fact that since we were studying non-fatiguing contractions, we had to have conditions which will not induce, in short time durations, localised muscle fatigue to set in.

There were five males, (ages 25-27 yrs., average height 1.65 m) as subjects in the first study, and the second study also had five males, (ages 26-28 yrs., average height 1.67 m). In both the cases, the subjects had no neuromuscular pathologies in their clinical histories. Written consents were obtained from all of these volunteers.

### 3.4.3. Test Procedure

In the first study, each subject was comfortably seated with his right arm secured at the two supports of the apparatus. He was asked to maintain the different joint positions for 10 seconds each. To avoid fatigue, sufficient rests ranging from 5 to 10 minutes were allowed in between two positions. Visual feedback of his forearm position with comparison to a reference line on the oscilloscope screen helped the subject maintain a particular joint position. The experiments were repeated once with a different sequence of positions maintained.

For the second study, the subject was secured to the apparatus as in the first case, and with a load (randomly selected) imposed, the subject then was to train himself moving the load at a particular angular velocity. Visual feedback of his forearm movement, as stated above, helped the subject maintain constant velocity movements. About 8 to 10 repetitions were done after the initial training period was completed. Rests ranging from 3 to 5 minutes were given between repetitions to avoid fatigue. The whole experiment was later repeated once. On the average two different loads or velocities were applied in any single session.

### 3.4.4. MES Detection

For comfortable, long term recording of the MES, non-invasive means of recording such as by surface electrodes must be employed. Although problems such as cross-talk from other muscles and electrode movement can cause low frequency noise to exist, these are minimised in our case with: the selection of the biceps brachii as our test muscle, the type of forearm movement involved (concentric motion of a supinated forearm) and the filtering scheme incorporated in the amplifier, which is detailed in the next section.

Two Ag/AgCl electrodes were paste coupled to the skin across the long axis of the muscle at a region midway between the cubital fossa and midpoint of upper arm (where the innervation zone of the biceps brachii is approximately located). The reason for doing so was obtained by perusing the results of Basmajian and De Luca [1] wherein they state that the region midway between the point of insertion and the innervation zone of the muscle yields a maximum level of MES activity. Before attaching the electrodes, the skin was abraded very well to reduce the skin-electrode impedance values to less than 8 k$\Omega$. The inter-electrode distance was 20mm and the overall position was maintained the same for a subject during all of his experimental sessions. It is important that interelectrode spacing be as consistent as possible to reduce signal bandwidth variations as noted previously [44]. The ground [reference] electrode was placed over the acromion of the right shoulder after abrading the skin at that region.

## 3.5. Analog Signal Conditioning

The MES detected as above, had a maximum amplitude of 4 mV. So a high gain bio-instrumentation amplifier (Nihon Kohden polygraph) was used for amplification to a range of $\pm 5$ Volts. After amplification, a bandpass filtering between 5 and 450 Hz was done to eliminate low frequency movement noise as well as to satisfy the Nyquist criterion. That is, the maximum bandwidth of the signal being sampled must be less than half the sampling frequency which in this case was 1 kHz. The differential input impedance of 10 MΩ with a CMRR of 80 dB served to keep distortion of the input MES to a minimum. The amplified signal to be processed using the computer had to be stored and faithfully reproduced off-line. For this purpose, the Tandberg Instrumentation tape recorder featuring frequency modulation was used with a tape speed of 3.75 inch/s and a signal to noise ratio of 60 dB.

## 3.6. Data Analysis

The data in analog form stored in the recorder had to be converted into digital form before processing it in the computer. For this purpose, a 12 bit analog to digital converter was used. However, the conversion and subsequent processing and analysis was performed using a software package called the 'Interactive Laboratory System' [ILS] and available on the VAX 11/780, which was the mainframe used in this study.

Thus, through ILS, the analog data stored in the FM tape recorder was digitised at a rate of 1000 samples/second and stored in the ILS domain as record files which list the digitised data alongside their sampling instants. For data manipulation during processing or analysis, each such record file was subdivided into several frames, each frame containing a few hundred samples. For the second study, only those data records which corresponded to the movement of the forearm between the angles of 120 and 80 degrees were considered for analysis. The reason for doing so, was that since this study was to effect constant velocity conditions, those segments of the signal which corresponded to acceleration or decelaration were not to be considered.

### 3.6.1. Pre-Analysis

Usage of power spectral analysis for MES requires it to be at least weakly stationary; that is, the mean and the autocorrelation must both be time-invariant. To test for weak stationarity, two non-parametric (i.e., statistically distribution independent) statistical tests called the 'RUNS' and 'TRENDS' tests detailed by Bendat and Piersol [3] were used. These tests are based on the notion that the statistical properties (the mean and the variance) computed by time averaging over each of a sequence of short segments into which a sample time history record is divided, will not vary significantly from one segment to another if the data is stationary. The RUNS test is valid for testing for long term variation while the TRENDS test is for short term variations.

Nearly all (182 out of 190) of the data records proved to be weakly stationary. Hence, the power spectral analysis of the stationary records could be performed. The next section details the estimation procedures employed.

### 3.6.2. Power Spectral Estimation

Of the various methods of power spectral analysis detailed in appendix A, two time tested and proven ways of spectral estimation for both short and long time records were chosen. These were the Blackman-Tukey (B-T) method and the Welch's method. Initially, only the B-T approach was used for the first study. Subsequently, the Welch's method was applied to all of the records of the second study along with a re-analysis of the spectral estimation for the first study by the same method. The re-analysis was done to compare the results obtained by the two methods. Incidentally, hardly any difference existed (by way of either the median frequency or the spectral power) between the spectra so estimated.

In the B-T method, as stated in the appendix, the maximum number of lags was made to be 1/20th of the number of values in the record file. Specifically, each of the data records being 10 seconds long, the autocorrelation was computed for 500 milli-seconds. Upon autocorrelation and subsequent fast Fourier transformation with a Hamming window, the power spectra were obtained for each of the records.

For the Welch's method, each of the segments (the size of the segment depending upon the width of the data) into which a record file was divided into, had its power spectrum estimated by squaring the FFT values of the Hamming windowed samples and by averaging the power spectra in the manner detailed in the appendix to yield the final spectrum. For the data records pertaining to the first study (10 secs long) the number of segments used were 20. In the second study, the number of segments were 8 to 10, the segment size ranging from 1 second for the 40 deg/sec case to 250 milli-seconds for the 160 deg/sec case. Both the methods discussed here are listed as Command Procedures (on the VAX 11/780) in appendix B.

Once the power spectra were obtained, their median frequencies and spectral powers were computed. This was done as follows. The power spectra were integrated between 0 and 500 Hz and the integrated value so obtained yielded the spectral power. The frequency which corresponded to an integrated value equal to half of the total gave the median frequency. Thus the median frequencies and the spectral powers were computed and tabulated for later analysis.

## 3.7. Review of the Assumptions Made

Several assumptions have been implicitly made in the experimental protocol detailed above. The significant ones amongst them are enumerated below.

The contribution of the torque due to the weight of the forearm segment to the external applied torque is assumed to be constant, in both the studies, for any single subject. Since we are interested in noting the relative spectral changes with the test parameters, this assumption is, therefore, plausible.

Though, in the flexing of the supinated forearm, the biceps brachii takes the major load, the other two flexor muscles, viz., the brachialis and the brachioradialis, also share some of the load. However, the detected surface MES is assumed to be manifested from the biceps brachii alone. The validity of this assumption is given by Patla et al. [38].

Lastly, changes in the velocity or the position of the forearm segment, which are what are actually measurable using the experimental scheme employed, are assumed proportional to that of the test muscle. This is a valid assumption considering the specific experimental objectives and constraints pertaining to these two test variables.

## 3.8. Summary

The experimental protocol, the choices of the various aspects of it, like the test parameters, the test muscle, the apparatus etc., all have been detailed in this chapter. Also some of the significant assumptions that were implicitly made in this protocol have been briefed. The power spectral estimation procedures which were chosen in this work have been discussed in terms of the signal processing software (ILS) employed for implementing the same.

In short, this chapter details the data collection and the data processing aspects of the work reported in this thesis. Analysis of the results so obtained after the processing, along with a discussion of the same, follows in the forthcoming chapters.

# Chapter 4
# RESULTS

The experimental aspects of the two studies reported in this work have been discussed in detail in the previous chapter. The median frequencies and the spectral powers computed with reference to applied torque, the angular velocity of contraction and change in joint angle (muscle length) as obtained for all of the subjects are recorded in tables in appendix C. The statistical analysis of those data are detailed with the aid of figures in the following sections.

## 4.1. Spectral Changes with Joint Angle

Herein is the analysis of the results obtained in the first study which, as mentioned before, consists of two cases (for the two loads, 19.6 and 29.4 N). The typical power spectra obtained, in one of the cases (29.4 N) for two different joint angles are illustrated in Figure 4-1. The magnitudes are in a normalised scale (to the maximum value obtained) to aid comparison. A frequency shift of the spectra as well as a magnitude change are readily observable.

The spectral power variation with joint angle for the first case is illustrated in Figure 4-2 below. The term average normalised power needs some explanation here. For any particular subject, the set of spectral power values obtained are normalised to the maximum amongst them to get the pattern of

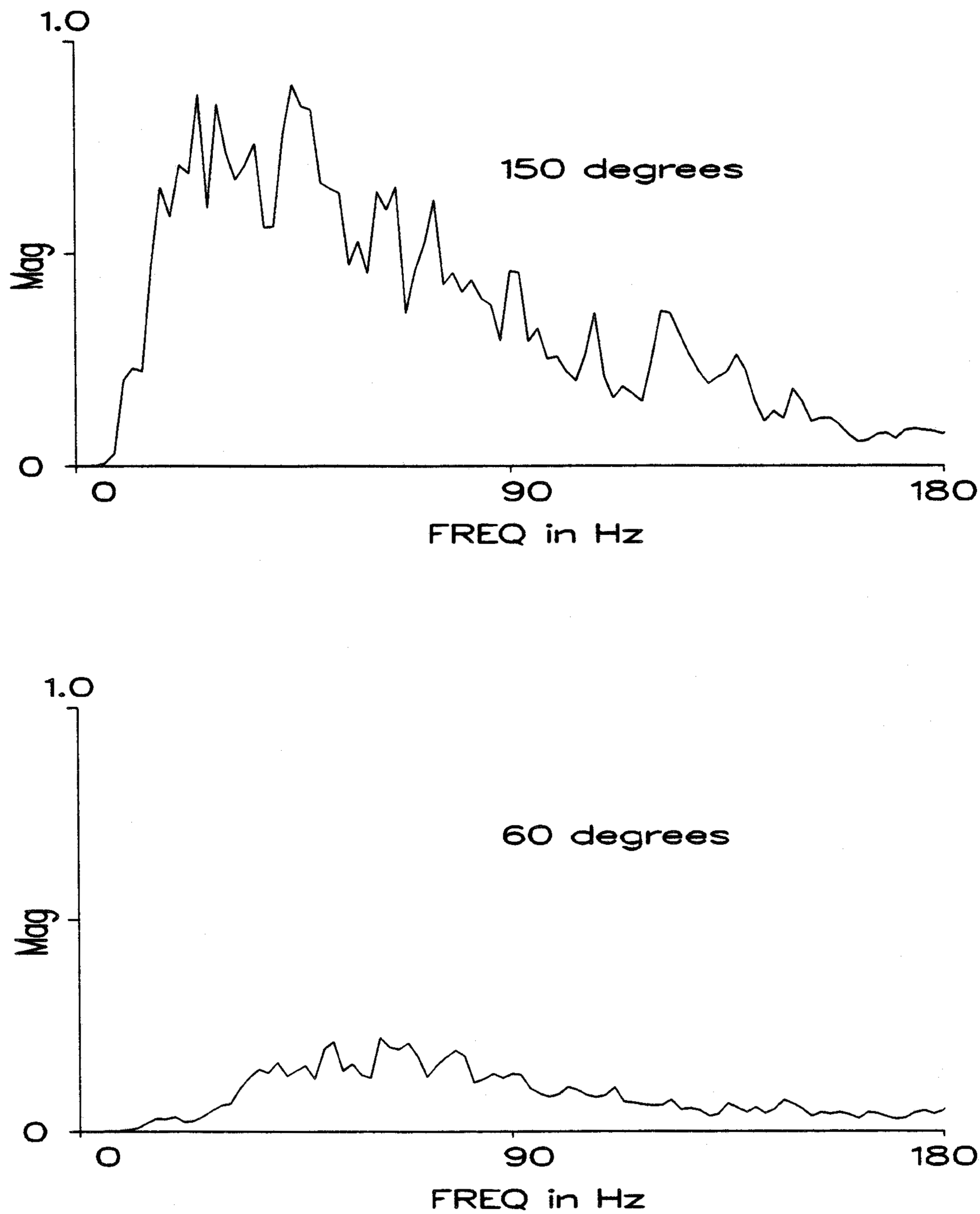


**Figure 4-1:** Typical Power Spectra obtained for two different Joint Angles with a load of 29.4N

variation of the test parameter for that subject. Similarly, such sets of normalised values are obtained for the other subjects too and then averaged to arrive at the average normalised power values. The spectral power is seen to have a concave depression to the top, the minimum being around $90^\circ$ joint angle. Studying the lever arrangement of the muscle with the forearm and upperarm would make us expect that a greater muscular effort (and hence a greater electrical activity) would be required to lift a load placed at the wrist level at angles other than $90^\circ$. The results obtained indeed confirms our expectation.

The median frequency values (again the average across the five subjects) are shown varying with joint angle in the Figure 4-3 below. The eight joint angles spaced only 15 degrees apart from near full extension ($165^\circ$) to approximately full flexion ($60^\circ$) are sufficient enough to justify interpolation of the results in between the tested angles.

Case 2 of the first study which involved three joint angles ($150^\circ$, $90^\circ$ and $60^\circ$) tested with five subjects for a load of 29.4 N was performed for confirmation of the results obtained in the previous case. Further explanation as regards this comparison is provided in the next chapter. However, the magnitudes of the average median frequency across the five sujbects for the three joint angles are depicted along with those obtained for the same angles in the previous case, for comparison purposes, in Figure 4-4 below.

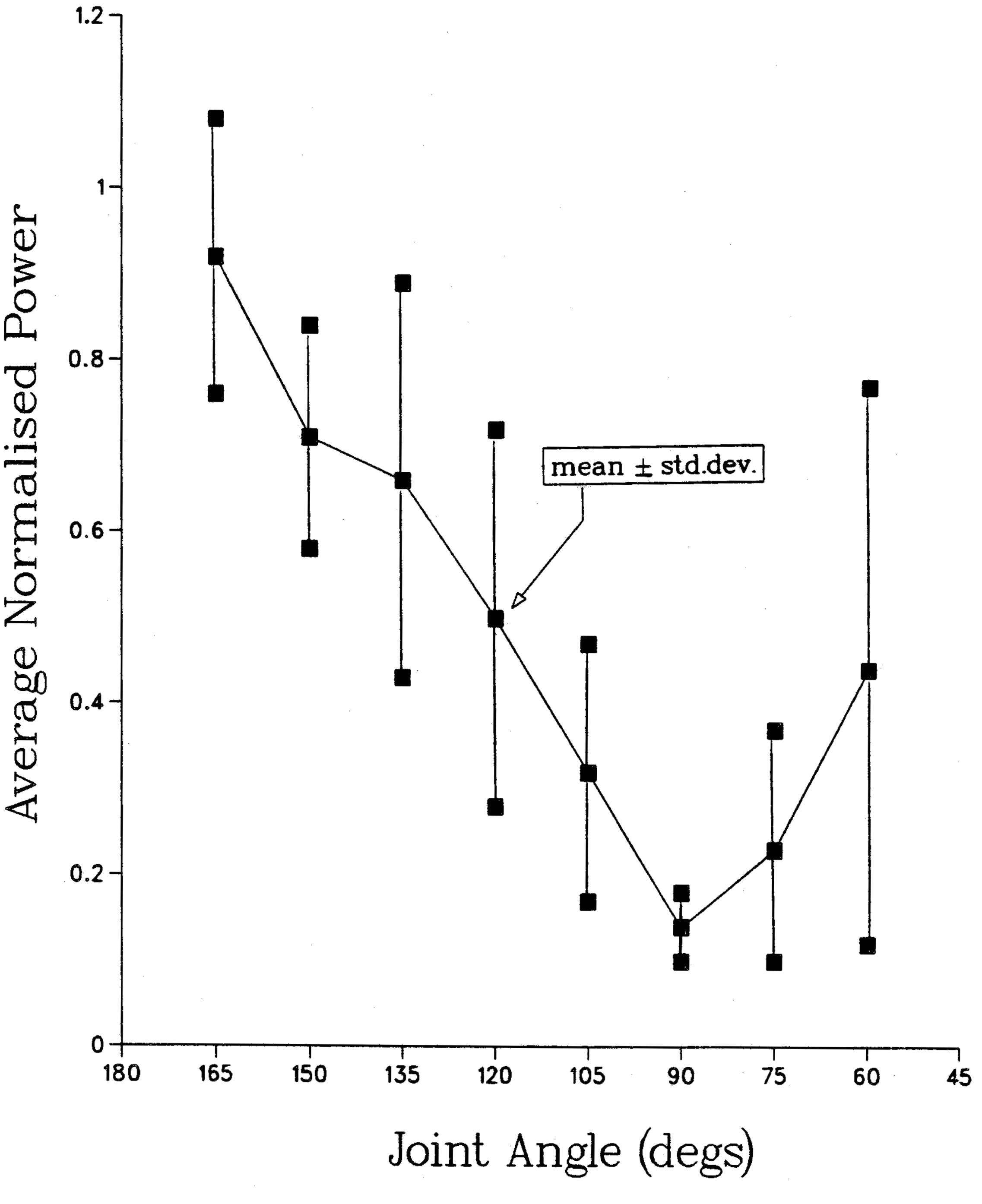


**Figure 4-2:** Spectral Power variation with Joint Angle

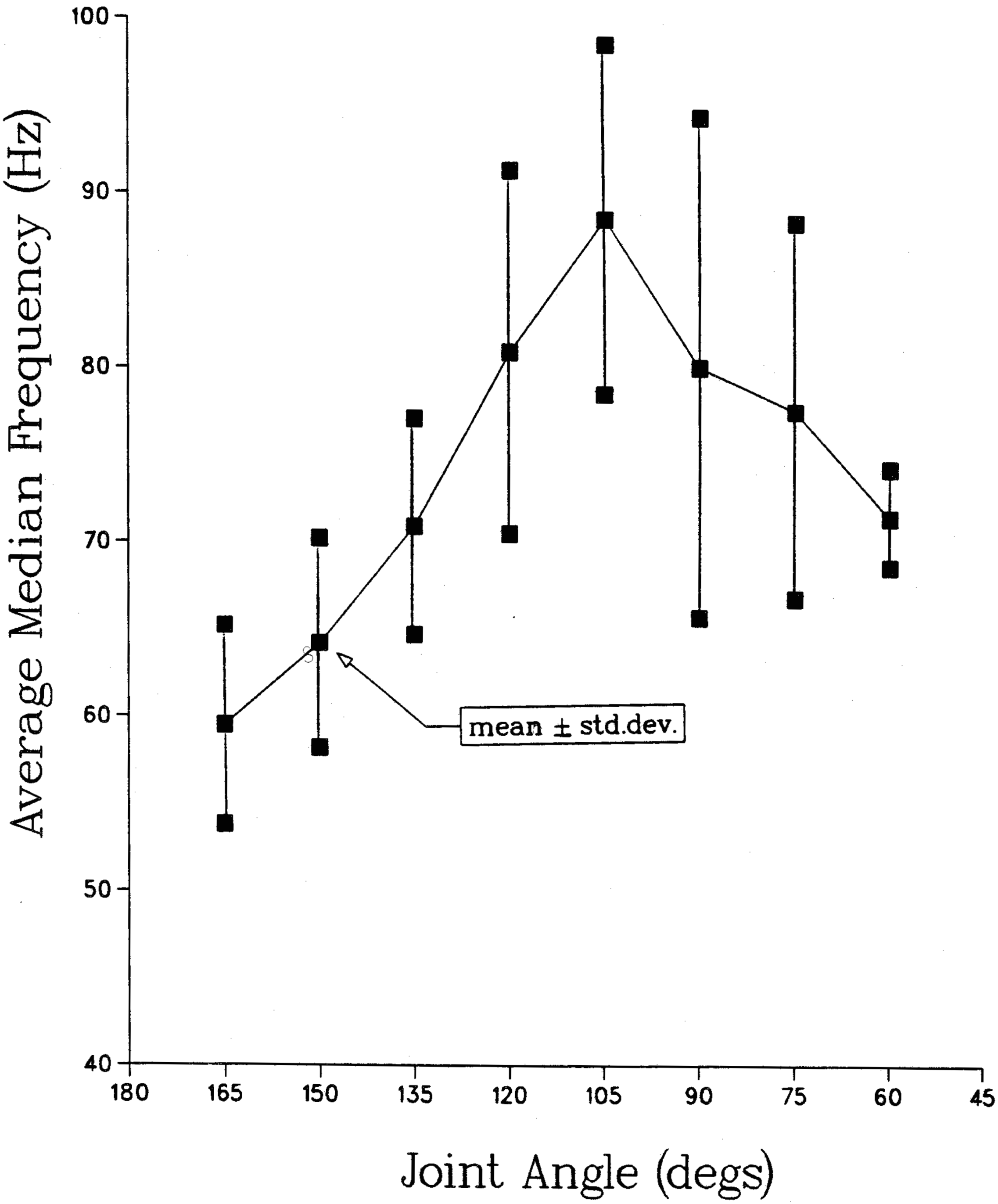


**Figure 4-3:** Median Frequency variation with Joint Angle

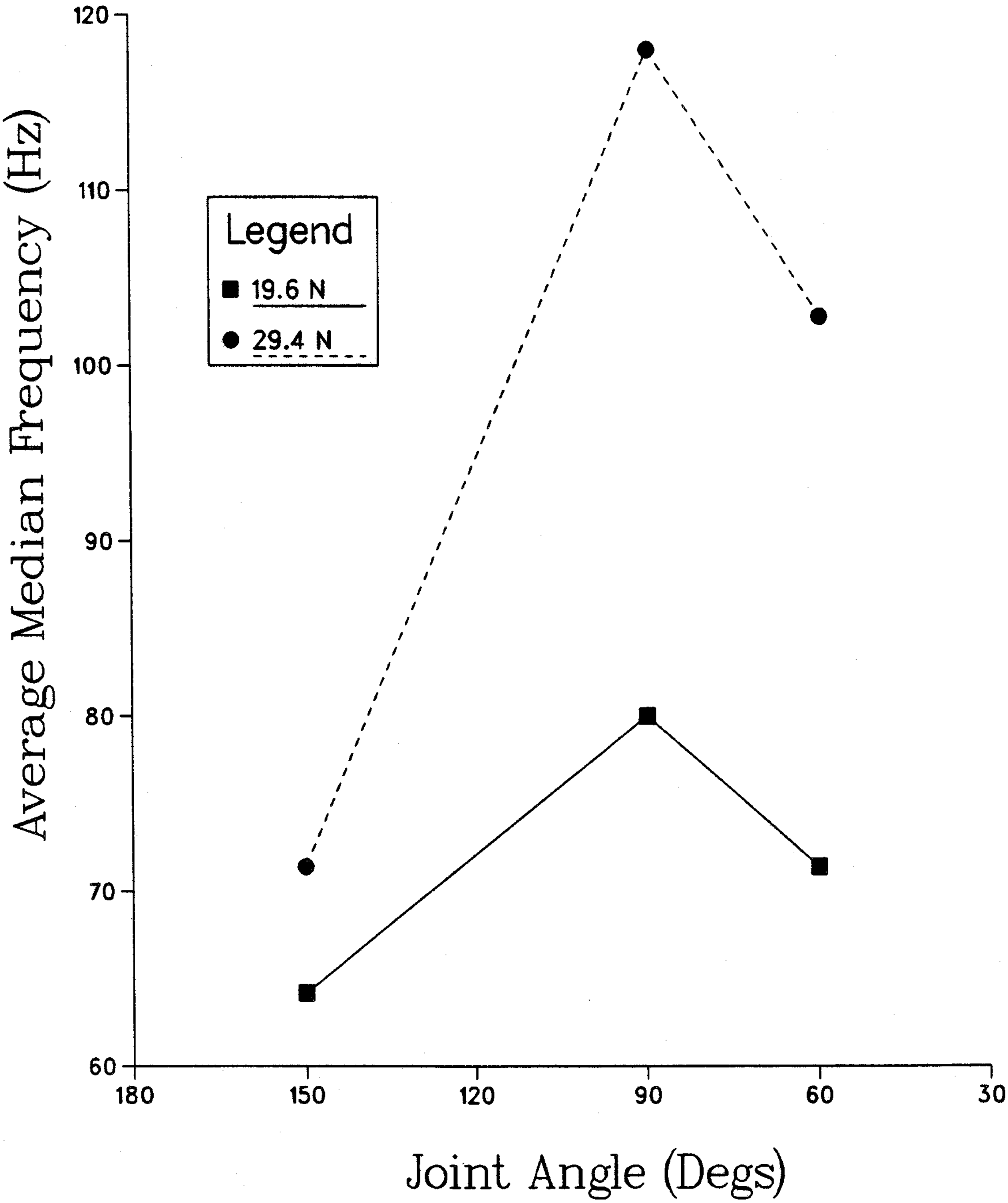


**Figure 4-4:** Comparison of Median Frequency values of the two cases

## 4.2. Spectral Changes with Applied Torque and Velocity

Studies on static contractions had revealed, as mentioned earlier, that the median frequency varies as a function of torque. It was therefore hypothesised, to start with, that not only the applied torque but also the angular velocity of contraction would cause changes in the median frequency. The experiments were set up, therefore, as constant velocity contractions with a variable applied torque and the experimental sessions repeated with different velocities. Before doing that, the spectral powers were to be correlated with the changes in both the said parameters, so that the expected linear correspondence (the mechanical power directly proportional to the electrical output) could be checked. As mentioned in chapter 3, the data analysed were of the contraction range of joint angle 120 to 80 degrees. The results for each of the subjects and for all of the torque-velocity combinations are recorded in Tables C-5 to C-14 in appendix C. Typical power spectra obtained for variations with torque with angular velocity constant and vice versa are illustrated in Figures 4-5 and 4-6. Figures 4-7 and 4-8 both illustrate the expected linear correspondence between the spectral power (average normalised power) and the torque and the velocity of contraction.

The average median frequency across the five subjects varies with the applied torque and the angular velocity of contraction as shown in Figure 4-9.

Since the experiments conducted in the second study involved both the torque and velocity parameters intertwined, it was felt appropriate to analyse both their effects simultaneously upon the median frequency. Thus, a stepwise

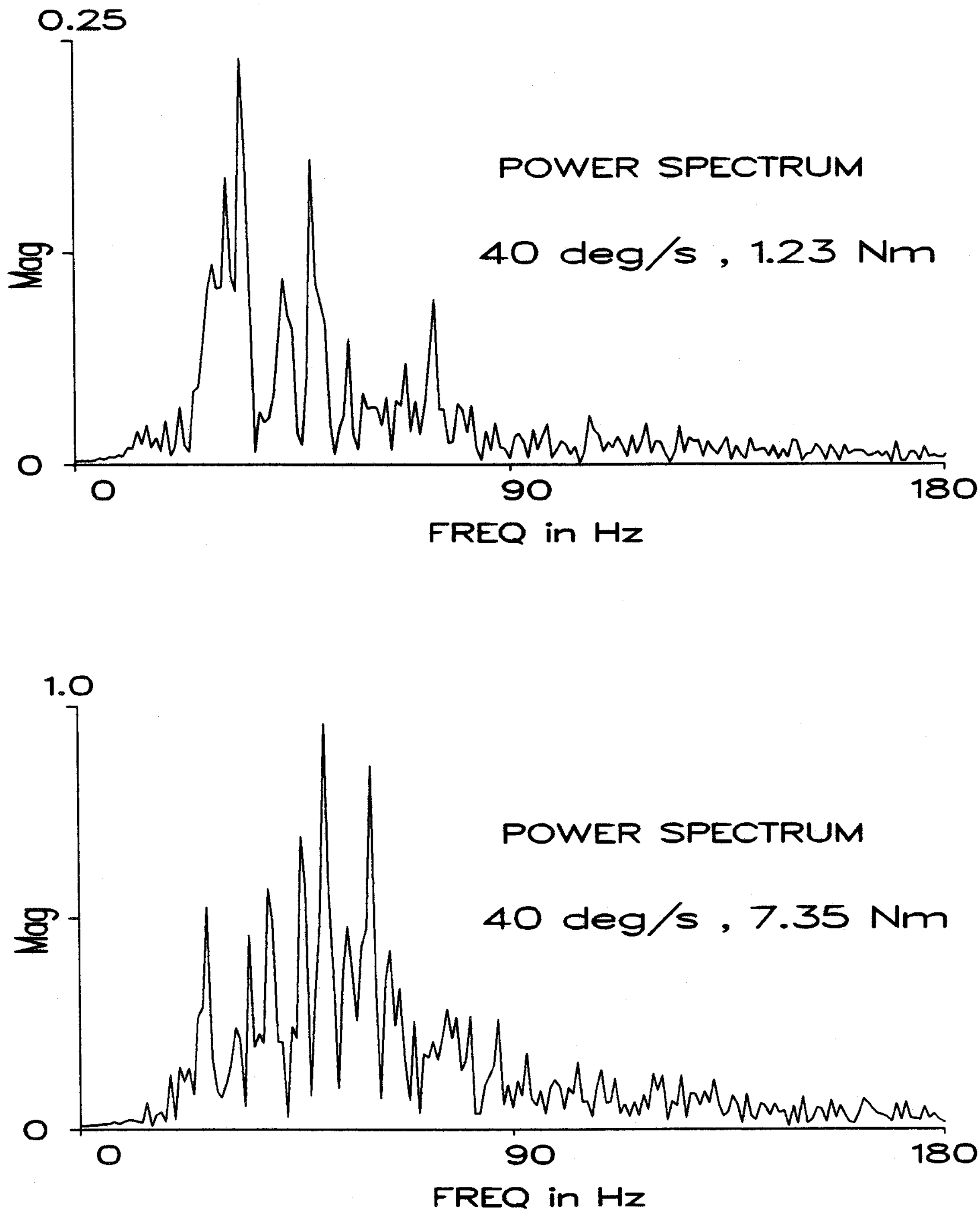


**Figure 4-5:** Typical Power Spectra obtained for two different Torques at the same Velocity of Contraction

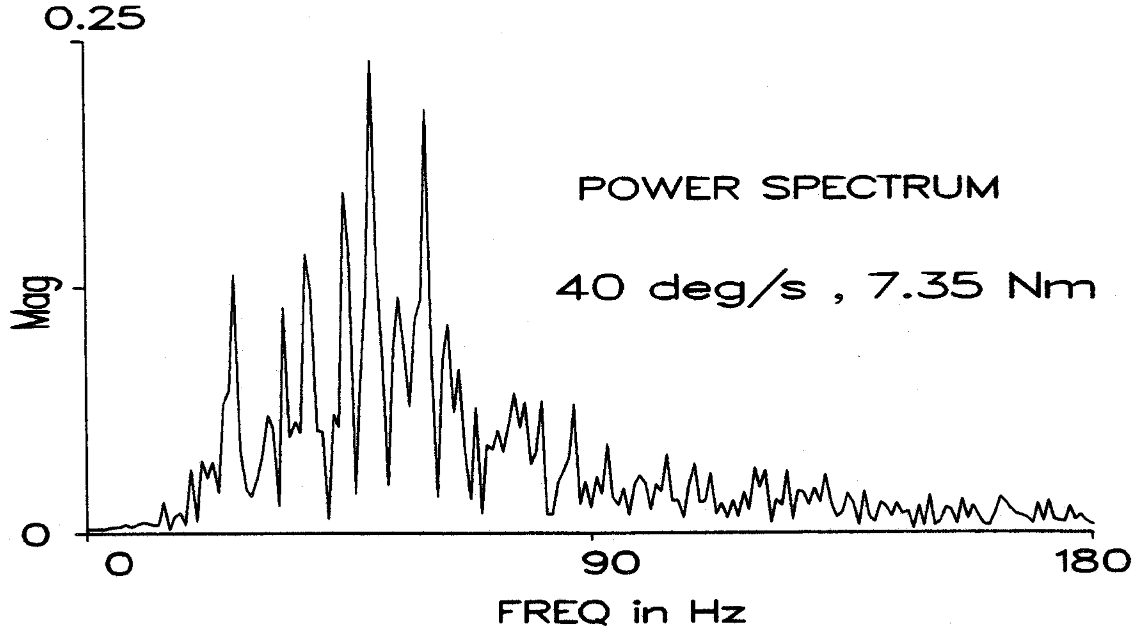


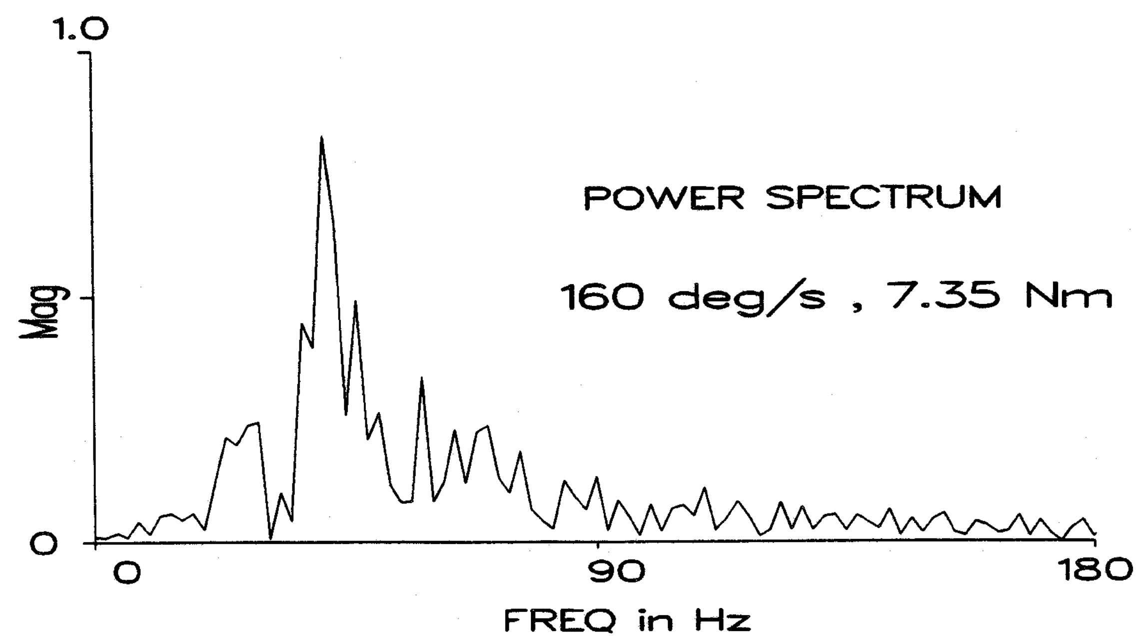


**Figure 4-6:** Typical Spectra for two different Velocities at the same Applied Torque

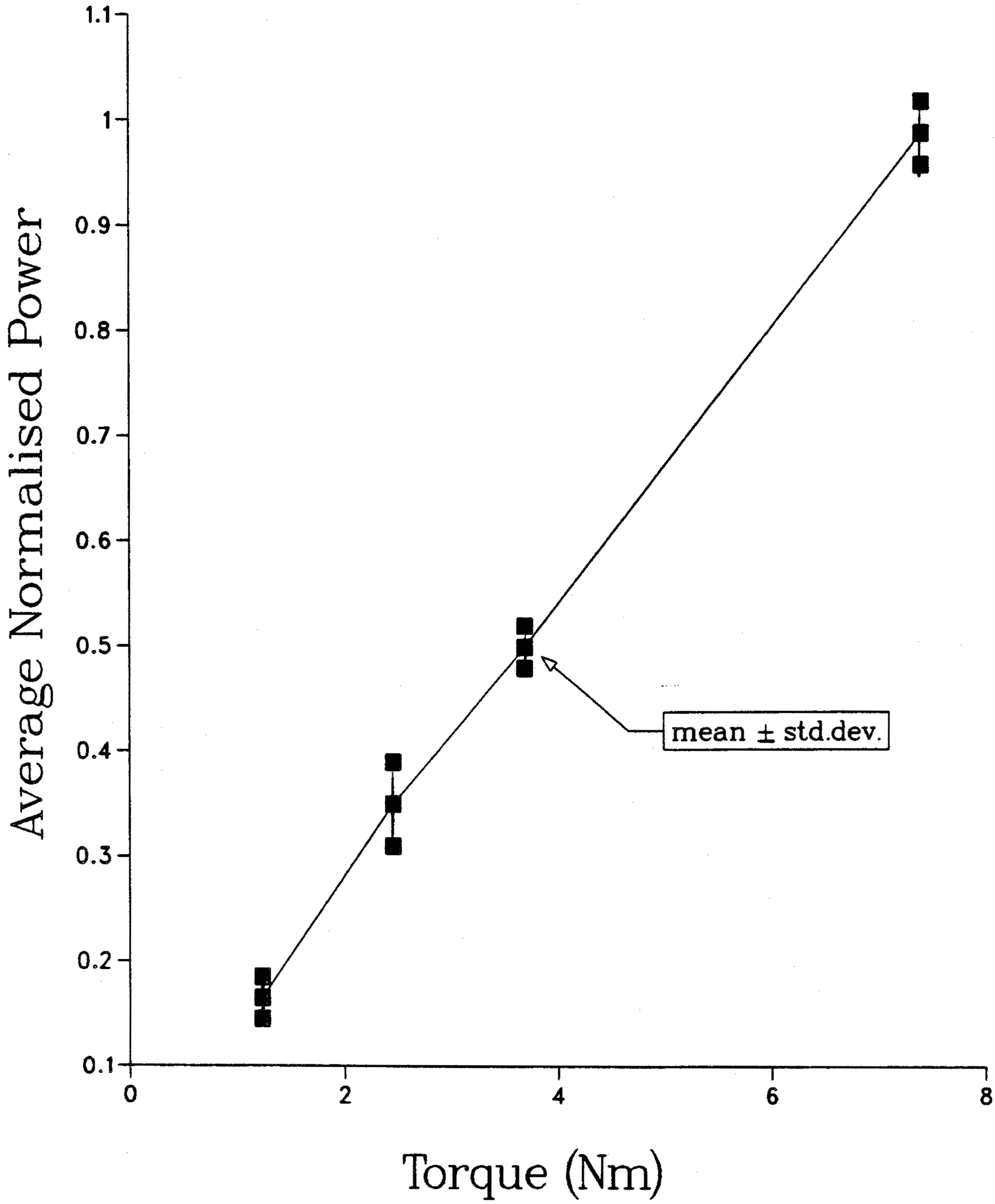


**Figure 4-7:** Variation of Average Normalised Power with Torque

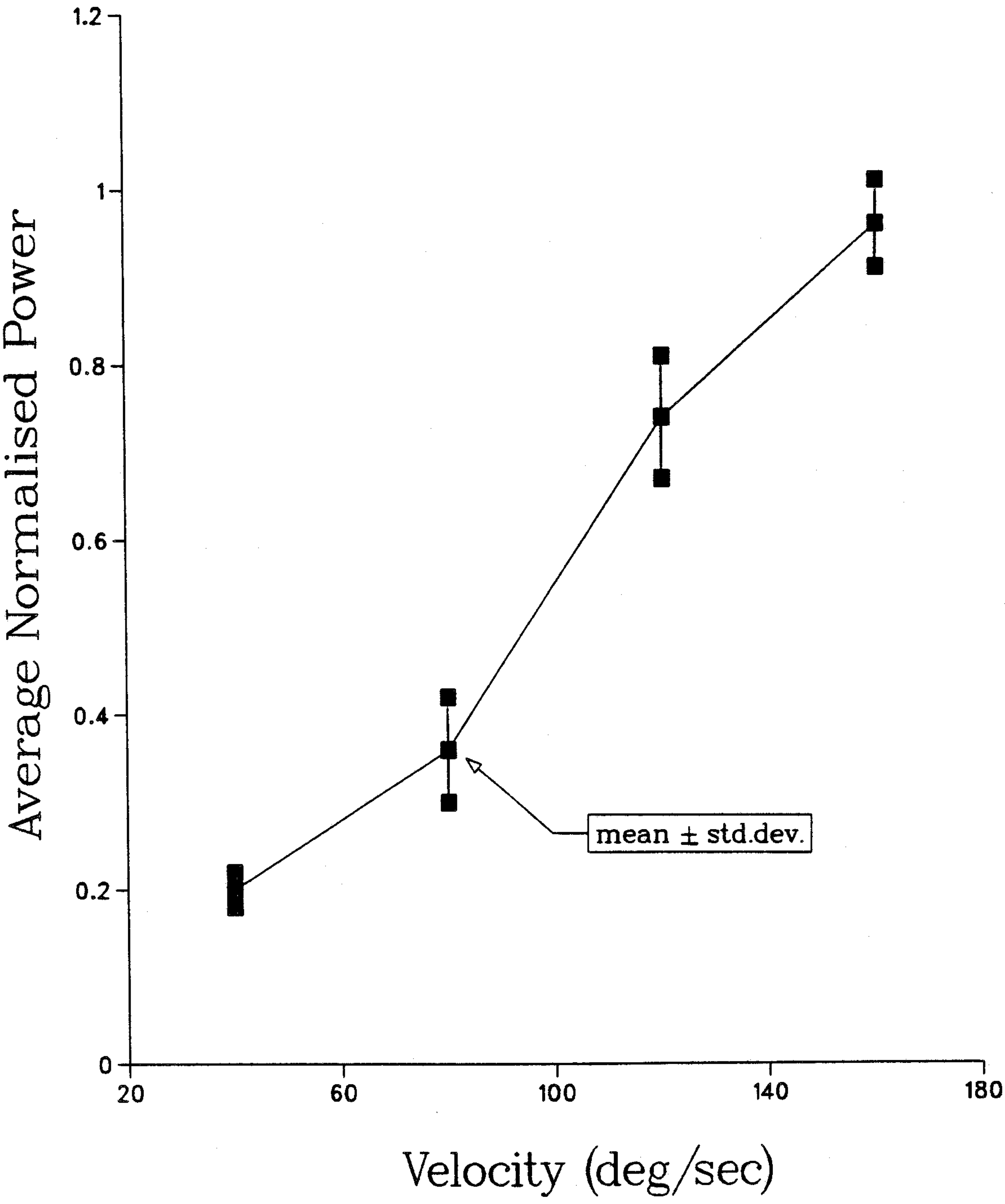


**Figure 4-8:** Variation of Average Normalised Power with Velocity

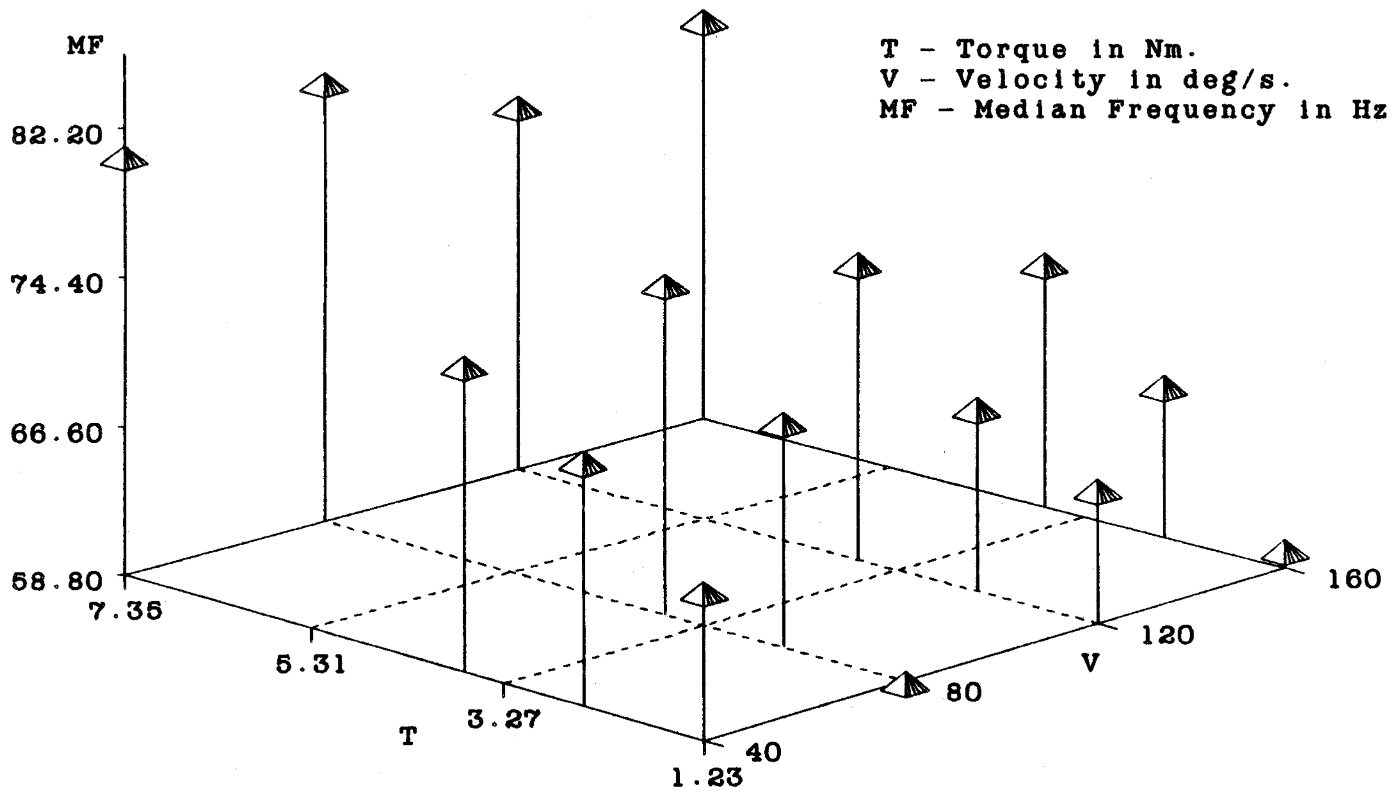


**Figure 4-9:** Plot of Median Frequency against Torque and Velocity

regression analysis was performed with the median frequency as the response variable and the torque, the angular velocity and their product (torque times the velocity) as the independent variables. The repetitions of the experiments were also taken into consideration as was the inter-subject variability by incorporating dummy variables into the analysis. The stepwise regression analysis accepted only the torque and the velocity variables as causing any significant changes in the response variable. The regression analysis yielded the following equations for the five subjects:

$$\text{Med.Freq.} = C + 2.9636*\text{Torque} - 0.0366*\text{Velocity},$$

$$\begin{aligned}\text{Where, } C &= 49.864 \text{ for subject } 1\\ &= 55.708 \text{ for subject } 2,\\ &= 80.083 \text{ for subject } 3,\\ &= 63.020 \text{ for subject } 4, \text{ and}\\ &= 69.333 \text{ for subject } 5.\end{aligned}$$

The estimates of this regression equation, as derived for one of the subjects, are given in a tabular form in appendix C. A discussion of the results obtained as detailed in the foregoing sections along with some speculations as to their behaviour follows in the next chapter.

# Chapter 5
# DISCUSSION

Upon perusing the several figures in the previous chapter, one can note that the surface MES power spectrum exhibits significant behaviour with the joint angle (and hence, muscle length), the applied torque and the angular velocity of contraction. A detailed discussion of these changes follows in this chapter.

## 5.1. Spectral Power Changes

The spectral power, which is the area beneath the power spectral curve and proportional to the average power of the myoelectric signal, varies as expected with all the three parameters studied. A linear variation with the applied torque and the angular velocity of contraction (as shown in Figures 4-7 and 4-8) reiterates the fact that the myoelectric activity is proportional to its mechanical counterpart. Also these linear relationships seem to indicate that neither the brachialis nor the brachioradialis are modifying the load upon the biceps brachii over the ranges of the applied torque and the velocity of contraction. The third class lever arrangement of the elbow joint with the biceps brachii and the applied load causes the spectral power output to vary with the joint angle as noticed in Figure 4-2. In the time domain, Miwa and Matoba [34] studying the myoelectric activity in the same muscle have similar observations.

## 5.2. Median Frequency Changes

### With Joint Angle

The median frequency has been noted to linearly increase with a decrease in joint angle by both Inbar et al., and Bazzy et al. But their results are based on only two or three joint angles and which are insufficient to correctly determine a relationship. In this work, eight joint angles placed 15° apart, from near full extension to approximately full flexion is sufficient enough to note in a detailed manner, the dependence of the median frequency on the joint angle. Though, as shown in Figure 4-3, there does exist a linear variation of the median frequency from a joint angle of 165° to 105°, there is also a downward shift beyond this range up to 60°.

When the supinated forearm is flexed, the diameter of the muscle fibers of the biceps brachii increases. Also there occurs a thinning of the fatty layer interposing between the skin and the muscle. Now, an increase in muscle fiber diameter causes an increase in action potential conduction velocity. The latter is related to the MES power spectrum by the following relation:

$$P(f)=\{\frac{1}{v^2}G(\frac{kfd}{v})\}$$

where 'v' is the conduction velocity of the active muscle fibers and 'G' is the shape function which is implicitly dependent on many anatomical, physiological, and experimental factors; and 'd' is the inter-electrode distance of the bipolar electrodes [1]. An increase in conduction velocity is noted to cause increased high frequency content and hence an increase in the value of the median frequency. Also, the distance-dependent, low-pass filtering effect would, as mentioned in chapter 2, effect less high frequency filtering due to the thinning of the interposing fatty layer. Both the factors, therefore would cause an increase in median frequency as was observed between the angles 165° and 105°. Beyond 105°, however, the fact that the median frequency tended to decrease entails further investigation. It could be hypothesised, for example, that an elastic compression of the muscle takes place at angles less than 90° which may distort the relationship between the median frequency and the joint angle.

However, to confirm that the observed relationship is a true one and not due to any random cause, the experiment was repeated, as mentioned before, with three joint angles (case 2 of study 1) but with an increased load of 29.4 newtons. It has been previously noted that in static contractions, an increase in applied torque causes an increase in median frequency at any of the joint angles*. If our observation is of a repeatable nature, then for the new load, a similar relationship should occur though with increased magnitudes. Indeed, this is what is noticeable upon perusing Figure 4-4.

### With Applied Torque and Velocity of Contraction

The variation of the median frequency with the joint angle as was found above would cause one to speculate that underlying trends may cause the data records obtained during dynamic contractions, over the joint angle range 120 to 80 degrees, to be non-stationary. But, as mentioned before, upon performing the two non-parametric statistical tests, weak stationarity was confirmed in nearly

---

*Most of the studies pertain to a joint angle of 90 degrees.

all of the data records. To specifically check upon possible median frequency changes within the range observed, each of the data records (for the velocities 40 and 80 deg/sec) was divided into two segments, one corresponding to the range of 120 to 100 degrees while, the other corresponded to 100 to 80 degrees. Their individual spectra were computed and also the median frequencies. Neither a significant (< 4 Hz) nor a systematic change was observed in the median frequency values between the two segments. A typical set of values obtained for one of the subjects is shown in Table 5-1. No such test was however performed for the higher velocity cases because of the danger of arriving at very low resolution and high variance estimates of the segmental spectral values.

| T / V | 40 | | 80 | |
|---|---|---|---|---|
| | 120-100 | 100-80 | 120-100 | 100-80 |
| 1.23 | 70 | 71 | 83 | 87 |
| 2.45 | 82 | 81 | 88 | 89 |
| 3.68 | 94 | 96 | 90 | 90 |
| 7.35 | 95 | 92 | 94 | 97 |

**Table 5-1:** Median frequency values obtained for subject no.3 for the two angular ranges

From Figure 4-9 which records the variation of the average (across the five subjects) median frequency with the torque and velocity, one observes that there does exist a linear trend in the median frequency with increase in applied torque though this is not so in the case of the velocity of contraction (the inter-subject variability and experimental errors may account for the perturbations in the observed trends). The biceps brachii with around 770 motor units [1] is a relatively large muscle. It has been observed that in large muscles, the recruitment process is the predominant way of accomodating an increase in load [23]. Now the recruitment process has been consistently observed to follow the 'size' principle; that is, for lesser loads, smaller motor units (smaller threshold too) are recruited, while, for increasing load, the larger motor units with greater thresholds become active. In the biceps brachii, the smaller threshold motor units are located deep within the muscle while the larger ones are located on the surface [42]. The surface MUAPs suffer less high frequency filtering, and hence, a median frequency increase would be observed (which is so in our case) with an increase in applied torque. A similar observation is made by Hagberg and Ericson [15] with regard to static contractions.

Now, the velocity of contraction covers a significantly wide range of values. It is intriguing that no significant trend was observed as regards the median frequency though the spectral power exhibited a linear relation. The regression analysis, the estimates of which are given in appendix C, confirms this. Now, an increase in the angular velocity of contraction could be visualised as an increase in the mechanical work required of the muscle. Therefore, either the recruitment and/or the rate coding process must be effective to match the observed spectral power changes. If recruitment was at play, as was observed in the previous case, then distinct changes in the MUAP waveform would have occured resulting in changes in the power spectrum. Since this is not the case in our observations, an interaction with the rate coding process or the latter alone could be the active process. Intuitively, one could visualise the active motor units, the type and number corresponding to the applied torque, to increase their firing rate to accomodate an increase in velocity and thus according some justification to the observation made above. But changes in the firing rate could be detected, in the power spectrum, in the frequency range less than 40 Hz [7] (if indeed the 'subpeak' located in this range is an indicator of the average firing rate of the active MUs). All the power spectral records, therefore, were checked for distinct subpeaks. Although certain number of subpeaks were indeed found in all of the spectra mentioned above they were not systematically occurring (in their locations or in their magnitudes in the spectra pertaining to the experimental repetitions). As Boxtel and Schomaker [7] point out, in the limb muscles, the firing rates varying over a wide range as opposed to being of a more or less single value (as was noticeable by them in small muscles), may cause several subpeaks to appear and no systematic changes can, therefore, be observed. Again, the variations observed could have very well occured due to random causes in the estimation procedures. However, the non-occurrence of significant subpeaks in our spectra in no way refutes the observation made above regarding the firing rate accomodating the velocity changes, though it remains to be investigated further. It also remains to be proved whether the median frequency is affected significantly by the firing rate changes. In most of the cases wherein median frequency was observed to vary with applied torque, as was the case in this study too, the recruitment process has been cited to be a valid cause [15]. Although Gander and Hudgins [12] cite the firing rate to be an equally valid factor, again, they base their observations upon their locating distinct subpeaks and their (subpeaks) shifting with an increase in the applied torque. Apart from the above, no other satisfactory explanation is forthcoming at this stage of the investigation.

Lack of reports of work on similar grounds in the literature does not permit either confirmation or rebuttal of the results observed in this project. Comparisons with results obtained in static contractions and in time domain analysis of dynamic contractions are however made to a certain degree. In fact, to reiterate, this being the first study of its nature, it is not surprising that the above situation is seen to occur. A few suggestions as regards further work, along the lines described in this study, is set forth in the next chapter.

# Chapter 6
# CONCLUSIONS

The study detailed in this thesis has shown that the power spectrum of the surface myoelectric signal obtained from the biceps brachii m. is significantly affected by the applied torque on the muscle, its velocity of contraction and changes in its length.

Both the median frequency and the spectral power are observed to consistently vary with similar patterns in five different subjects with all the three parameters mentioned above. However, only more extensive investigations will ensure their being reliable indicators of such changes during dynamic contractions as they are in the static cases. A common pattern of variation may perhaps ensue from conducting similar experiments upon other muscles too.

As was mentioned in an earlier chapter, the two basic processes which are activated in a muscle to meet its mechanical requirements are 'recruitment' and 'rate coding'. To reiterate, recruitment refers to the neural stimulation of previously inactive motor units to meet a certain load requirement, while rate coding refers to increasing the firing rates of the already active motor units. The two either complement each other or one predominates over the other over a certain range of load beyond which the other takes over; the exact process of how or when one process augments or predominates over the other is not very clear till to date. In our case, the process of recruitment coupled with the low pass filtering effect due to the distance intervening between the muscle and the detecting electrodes is considered to satisfactorily explain both the median frequency increase due to the applied torque and its 'hump' like variation with a decrease in muscle length. The spectral power for both the torque and the muscle length is observed to follow the magnitude of the myoelectric activity accompanying a specific effort exerted by the muscle. In the same context, the velocity of contraction is strongly suggestive of affecting the firing rates of the active motor units suitably recruited for the desired load or torque. Further investigations, along theoretical or experimental lines, are needed to reveal a more definitive relationship between a muscle's velocity of contraction and its power spectrum. Extension of the experimental protocol used in this work onto eccentric contractions is seen to be another logical step ahead.

Both the spectral estimation techniques employed in this work have proved to be satisfactory in obtaining significant information from the power spectra. In attempting to use higher values of the velocity of contraction than the range employed in this study, both the methods, however, are limited because, the frequency resolution obtainable through their usage is inversely proportional to the data record length and which is undesirable. In this regard, the advantages of employing modern spectral analysis methods to help overcome this problem, as has been suggested by a few researchers, is debatable.

The biceps brachii as the test muscle turned out to be a wise choice since the knowledge of its biomechanical characteristics in relation to myoelectric activity helped correlate our observations with the underlying physiology. Its lever arm and the hinge movement of the elbow joint proved to be advantageous in that a simple forearm loading apparatus like the one designed and used in this study would hardly introduce any errors into the characteristics of the data collected and also not interfere in the process of the data collection itself.

One of the reasons that static contractions have been widely studied in the frequency domain is that they are easily controllable as regards the number of test conditions to be imposed and the experimental protocol that pertains to them, since only the varying force or torque need be considered. Also as regards spectral analysis, it was feared that perhaps the surface manifested myoelectric signal in a dynamic contraction would be non-stationary and hence prove to be difficult to analyze. It was largely due to these two reasons that dynamic contractions have been neglected in the spectral domain. In fact, to the author's knowledge, this is the first work pertaining to study of the spectra obtained during dynamic contractions which included the velocity of contraction. To that effect, this study has made a small but surely significant contribution in analysing a muscle's dynamic nature and in bringing about a sense of completeness in the analysis of the myoelectric signal in the frequency domain.

# REFERENCES

**1**. Basmajian J.V. and De Luca C.J.. *Muscles Alive*. William and Wilkins, 1985.

**2**. Bazzy, A.R., Korten, J.B. and Haddad, G.G. "Increase in Electromyogram Low-Frequency Power in Non-Fatigued Contracting Skeletal Muscle". *Journal of Applied Physiology 61*, 3 (1986), 1012-1017.

**3**. Bendat, J.S. and Piersol, A.G.. *Measurement and Analysis of Random Data*. John Wiley and Sons, 1966.

**4**. Bigland, B and Lippold, O.C.J. "The relation between Force, Velocity and Integrated Electrical Activity in human muscles". *Journal of Physiology (London) 123* (1954), 214-224.

**5**. Blinowska, A., Verroust, J. and Cannet, G. "An Analysis of Synchronization and Double Discharge Effects on on Low Frequency Electromyographic Power Spectra". *Electromyography and Clinical Neurophysiology 20* (1980), 465-480.

**6**. Bouisset, S and Goubel, F. "Interdependence of relations between Integrated EMG and diverse biomechanical quantities in normal voluntary movements". *Activitas Nervosa Superior 13* (1971), 23-31.

**7**. Boxtel, A.V. and Schomaker, L.R.B. "Motor Unit Firing Rate during Static Contraction indicated by the Surface EMG Power Spectrum". *IEEE Transactions in Biomedical Engineering 30*, 9 (1983), 601-609.

**8**. Childers, D.G., Aunon, J.I., and McGillem, C.D. "Spectral Analysis: Prediction and Extrapolation". *CRC Critical Reviews in Bioengineering 6* (1981), 133-176.

**9**. Clamann, H.P. and Broecker, M.S. "Relation between Force and Fatiguability of Red and Pale Skeletal Muscles in Man". *American Journal of Physical Medicine 58* (1979), 70-85.

**10**. Danoff, J.V. "The Integrated Electromyogram related to Angular Velocity". *Electromyography and Clinical Neurophysiology 19* (1979), 165-174.

**11**. De Luca, C.J. "Physiology and Mathematics of Myoelectric Signals". *IEEE Transactions on Biomedical Engineering 26*, 6 (1979), 313-325.

**12**. Gander, R.E. and Hudgins, B.S. "Power Spectral Density of the Surface Myoelectric Signal of the Biceps Brachii as a function of Static Load". *Electromyography and Clinical Neurophysiology 25* (1985), 469-478.

**13**. Gydikov, A. and Kosarov, D. "Some features of different Motor Units in Human Biceps Brachii". *Pflugers Archives 347* (1974), 75-88.

**14.** Hagberg, M. "The Amplitude Distribution of Surface EMG in Static and Intermittent Static Muscular performance". *European Journal of Applied Physiology 40* (1979), 265-272.

**15.** Hagberg, M. and Ericson, B.E. "Myoelectric Power Spectrum dependence on Muscular Contraction Level of Elbow Flexors". *European Journal of Applied Physiology 8* (1982), 147-156.

**16.** Harris, F.J. On the Use of Windows for Harmonic Analysis with the Discrete Fourier Transform. Proceedings of the IEEE, 1978, pp. 51-83.

**17.** Inbar, G.F., Allin, J., Paiss, O. and Kranz, H. "Monitoring Surface EMG spectral changes by the Zero Crossing Rate". *Medical and Biological Engineering and Computing 24* (1986), 10-18.

**18.** Kadefors, R., Kaiser, E. and Petersen, I. "Dynamic Spectrum Analysis of Myo-potentials with special reference to Muscle Fatigue". *Electromyography 8* (1968), 39-74.

**19.** Kay, S.M. and Marple, S.L. Spectrum Analysis - A Modern Perspective. Proceedings of the IEEE, 1981, pp. 1380-1419.

**20.** Komi, P.V. Relationship between Muscle Tension, EMG and Velocity of Contraction under Concentric and Eccentric Work. In Desmedt, J.E., Ed., *New Developments in Electromyography and Clinical Neurophysiology*, Karger, Basel, 1973, pp. 596-606.

**21.** Kopec, J and Hausman-Petrusewicz, I. "Application of harmonic Analysis to the Electromyogram Evaluation". *Acta Physiologica Polonica 17* (1966), 598-608.

**22.** Kugelberg, E. "Electromyograms in Muscular Disorders". *Journal of Neurology and Neurosurgical Psychiatry 10* (1947), 122-123.

**23.** Kukulka, C.G., and Clamann, P.H. "Comparison of the Recruitment and Discharge Properties of Motor Units in Human Brachial Biceps and Adductor Pollicis during Isometric Contractions". *Brain Research 219* (1981), 45-55.

**24.** Kwatny, E., Thomas, D.H. and Kwatny, H.G. "An Application of Signal Processing Techniques to the study of Myoelectric Signals". *IEEE Transactions on Biomedical Engineering 4*, 17 (1970), 303-312.

**25.** Lago, P and Jones, N.B. "Effect of Motor-Unit Firing Time Statistics on E.M.G. Spectra". *Medical and Biological Engineering and Computing 15* (1977), 648-655.

**26.** Larsson, L.E. "On the relation between the EMG Frequency Spectrum and the duration of symptoms in lesions of the peripheral motor neuron". *Electroencephalography and Clinical Neurophysiology 38* (1975), 69-78.

**27**. Le Fever, R.S. and De Luca, C.J. The contribution of individual Motor Units to the EMG Power Spectrum. Proceedings of the 29th Annual Conference of Engineering in Medicine and Biology, 1976, pp. 41-45.

**28**. Lindstrom, L.R., Magnusson, R. and Petersen, I. "Muscular Fatigue and Action Potential Conduction Velocity changes studied with Frequency Analysis of EMG Signals". *Electromyography 4* (1970), 341-353.

**29**. Lindstrom, L.H. and Magnusson, R.I. Interpretation of Myoelectric Power Spectra: A Model and its Applications. Proceedings of the IEEE, 1977, pp. 653-662.

**30**. Lindstrom, L and Petersen, I. *Progress in Clinical Neurophysiology.* Volume 10: Power Spectrum Analysis of EMG signals and its applications. In Desmedt, J.E., Ed., *Computer-Aided Electromyography*, Karger, Basel, 1983, pp. 1-51.

**31**. McLeod, W.D., Nunnaly, H.N. and Cantrell, P.E. "Dependence of EMG Power Spectra on Electrode Type". *IEEE Transactions in Biomedical Engineering 3* (1976), 172-175.

**32**. Merletti, R, Sabbahi, M.A. and De Luca, C.J. "Median Frequency of the Myoelectric Signal: Effects of Ischemia and Cooling". *European Journal of Applied Physiology 52* (1984), 258-263.

**33**. Milner-Brown, H.S., and Stein, R.B. "The relation between the Surface Electromyogram and Muscular Force". *Journal of Physiology (London) 246* (1975), 549-569.

**34**. Miwa, N and Matoba, M. "Relation between the Muscle strength and Electromyogram". *Orthopaedics and Traumatology 8* (1959), 121-124.

**35**. Moritani, T and De Vries, H.A. "Reexamination of the relationship between Surace Integrated Electromyogram and Force of Isometric Contractions". *American Journal of Physical Medicine 57* (1978), 263-277.

**36**. Muro, M., Nagata, A., Murakami, M.D. and Moritani, T. "Surface EMG Power Spectral Analysis of Neuromuscular Disorders during Isometric and Isotonic Contractions". *American Journal of Physical Medicine 61*, 5 (1982), 244-254.

**37**. Naeiji, M. and Zorn, H. "Relation between EMG Power Spectrum shifts and Muscle Fiber Action Potential Conduction Velocity changes during Local Muscular Fatigue in Man". *European Journal of Applied Physiology 50* (1982), 23-33.

**38**. Patla, A.E., Hudgins, B.S., Parker, P.A. and Scott, R.N. "Myoelectric Signal as a Quantitative Measure of Muscle Mechanical Output". *Medical and Biological Engineering and Computing 20* (1982), 319-328.

**39.** Petrofsky, S.J. and Lind, A.R. "The influence of temperature on the amplitude and frequency components of the EMG during brief and sustained isometric contractions". *European Journal of Applied Physiology 44* (1980), 189-200.

**40.** Sato, H. "Functional Characteristics of Human Skeletal Muscle revealed by Spectral Analysis of the Surface Electromyogram". *Electromyography and Clinical Neurophysiology 22* (1982), 459-516.

**41.** Scherrer, J and Bourguignon A. "Evaluation electromyographique du travail statique". *Journal of Physiology (Paris) 49* (1957), 376-378.

**42.** Tesch, P. and Karlsson, J. "Lactate in Fast and Slow Twitch Skeletal Muscle Fibers of Man during Isometric Contractions". *Acta Physiologica Scandinavica 99* (1977), 230-236.

**43.** Welch, P.D. "The Use of Fast Fourier Transform for the Estimation of Power Spectra: A Method based on Time Averaging over Short, Modified Periodograms,". *IEEE Transactions on Audio Electroacoustics AU-15* (1967), 70-73.

**44.** Zipp, P. "Effect of Electrode Parameters on the Bandwidth of the Surface EMG Power Density Spectrum". *Medical and Biological Computing 116* (1978), 537-541.

# Appendix A
# POWER SPECTRAL ANALYSIS

The Power Spectrum or the Power Spectral Density Function (PSD) of random data describes the general frequency composition of the data in terms of the spectral density of its mean square value. It is defined as,

$$P(f)=\lim_{\Delta f\rightarrow 0}\frac{1}{\Delta f}[\lim_{T\rightarrow\infty}\frac{1}{T}\int_0^T x^2(t,f,\Delta f)dt]$$

where, x(t,f,Δ f) is that portion of the random data, x(t), in the frequency range from f to f+Δ f (Δ f is a very small value). The quantity P(f) is always a real valued and non-negative function. Also, since the term $x^2$ is the squared value of the random variable, say, a voltage, therefore, the power spectral density function could be thought of as the average power associated with a frequency bandwidth of 1 Hz (assuming f taking steps of 1 Hz) and centered at f Hz.

To better understand the power spectral estimation procedures, a review of the concept of 'autocorrelation function' is made below.

**Autocorrelation Function**

The autocorrelation function of random data describes the general dependence of the values of the data at one time on the values at another time.

Given a sample time history record x(t) and its value at $\tau$ units later, ($\tau$ is called the 'lag number') $x(t+\tau)$, the autocorrelation function in equation form is,

$$R(\tau) = \lim_{T \to \infty} \frac{1}{T} \int_0^T x(t)x(t+\tau)dt$$

where, T is the observation time.

If we consider a finite data sequence $\{x_k\}$, k=0,1,...,N-1, with the samples spaced $\Delta$ t apart, its autocorrelation function in discrete form is given by,

$$R(m) = \frac{1}{N-m} \sum_{n=0}^{N-m-1} x_{n+m} x_n$$

where, m, the lag number =0,1...p $\leq$ N-1.

The quantity $R(\tau)$ is always a real-valued even function with a maximum at $\tau$=0 and may be positive or negative. In equation form,

$R(\tau) = R(-\tau)$ and

$|R(0)| \geq |R(\tau)|$ for all $\tau$

An important property associated with the autocorrelation function lies in its relationship to the power spectral density function. Specifically, for stationary data, the two functions are related by a Fourier Transform as follows.

$$P(f) = 2\int_{-\infty}^{\infty} R(\tau) e^{-j2\pi f\tau} d\tau$$

Because $R(\tau)$ is an even function of $\tau$, therefore,

$$P(f) = 4\int_{0}^{\infty} R(\tau) e^{-j2\pi f\tau} d\tau$$

This relationship is called the 'Weiner-Khinchine' relation and is utilised in estimating the power spectra as will be noted in the next section.

## A.1. Power Spectral Estimation

Of the several methods that have been developed for estimating the power spectra, only some of the widely used procedures are discussed below, and they are classified either as traditional or modern methods of spectral estimation.

### A.1.1. Traditional Methods

#### A.1.1.1. Blackman-Tukey Method

Consider a weakly stationary process x{t} whose PSD function is to be estimated. The Weiner-Khinchine relation as mentioned above relates the PSD with the autocorrelation function as,

$$P(f)=4\int_0^{\infty} R(\tau)e^{-j2\pi f\tau}d\tau$$

Its discrete form is given by

$$P(f)=\Delta t \sum_{m=0}^{m=M} R(m)e^{-j2\pi f m\Delta t},$$

where, $\Delta t$ is the sampling interval and R(m), m = 0, . . . , M, are the discrete estimates of the correlation function.

The correlation coefficients are, therefore, first estimated from the sampled data record, x{k}, k=0,1, . . . , N-1, as shown in the previous section. Using the estimates of the correlation function thus obtained in the Weiner- Khinchine relation yields the power spectrum.

This method is computationally efficient and yields spectral records with a resolution approximately the inverse of the width of the autocorrelation lags.

The normalised square error, the ratio of the variance of the estimate to the square of the expected value,(defined later) is given by $\epsilon^2 = m/N$ where, $m$ is the maximum number of autocorrelation lags and $N$ is the number of data points being analysed. As a rule of thumb, the value of $m$ is suggested by Blackman and Tukey to be 10 to 20% of $N$.

### A.1.1.2. Welch's Method

The Welch's method is a modification of the Periodogram approach (wherein the power spectra is estimated by squaring the absolute values of the Fourier transform magnitudes and averaged over the period considered) to spectral estimation. Both the periodogram and the Welch's methods estimate the power spectra without first estimating the correlation function.

The Discrete Fourier Transform (DFT) of a finite sampled data sequence, $\{x_k\}$ is given by,

$$X(m) = \Delta t \sum_{k=0}^{N-1} x_k e^{\frac{-j2\pi mk}{N}}$$

Squaring the magnitude values of the DFT ($|X(m)|^2$) yields the periodogram. Since the squaring of the DFT magnitudes yields the energy distribution, scaling it down by $\Delta$ t (sampling rate), gives the power spectrum. That is,

$$P(f) = \frac{1}{N\Delta t} |X(m)|^2$$

Since, the original definition of the power spectrum involves an averaging over infinity, the above is, therefore, a poor estimate and hence would suffer from a large variance. Therefore, a modification was made by Welch [43]. His approach consists of dividing the data record into a number of equal segments (overlapped or non-overlapped) each of whose power spectrum is estimated as above. The average of these estimates (approximately over a long interval instead of an infinite one) would yield the final power spectrum and has been shown to be less prone to statistical variations.

Mathematically, the process can be explained as follows. Consider the sequence $\{x_k\}$, k=0,1, . . . ,N-1. We define segments of length 'L', such that the $i^{th}$ segment is given by the sequence,

$$x_k^{\,i} = x(k + (i-1)D),$$

where, k=0,1, . . . ,L-1
i=1,2, . . . ,K
D is the overlapping number of samples (zero for no overlap)

The periodograms of the K overlapped or non-overlapped segments are then calculated using the fast Fourier transform (FFT) which is nothing but a computer algorithm designed for a very fast computation of the DFT of a data record. Denoting the periodogram of the $i^{th}$ segment by $P_i[m]$, where,

$$P_i[m] = \frac{\Delta t}{L} \left| \sum_{k=0}^{L-1} x_k^{\,i} e^{\frac{-j2\pi mk}{L}} \right|^2$$

$i = 1,2, \ldots ,K$

the Welch's spectral estimate is given by the average of all K periodograms

$$P[m]=\frac{1}{K}\sum_{i=1}^{K} P_i[m]$$

The variance of the averaged power spectrum can be shown to be $(1/K)^{th}$ of that of the periodogram approach alone. Also the normalised square error is again $(1/K)^{th}$ of that obtained through the Blackman-Tukey method. The resolution is given by the inverse of the time width of a single segment.

### A.1.2. Some Comments on the Traditional Methods

The exact power spectral density function cannot, in general, be calculated. This is because the given signal is time limited, is often corrupted with noise and sometimes non-stationary too. Moreover, the usage of digital methods for efficient and fast computations requires the data to be sampled. Therefore, one can arrive only at 'estimates' of the power spectral density function. However, to quantify how close these estimates are to the true values, two important statistical measures are often used and these are:

1. **Variance of the Estimate**: Also known as 'Mean Square Error', it is defined as $Var[P']=E[(P'-P)^2]$, where, P' is an estimate of a true or expected value P and E is the expectation operator.

2. **Normalised Square Error**: Also called the 'quality ratio' this is the ratio of the variance to the square of the true or expected value. That is normalised square error, $\epsilon^2 = \dfrac{E[(P'-P)^2]}{P^2}$

Since we can process or analyse only finite duration signals, we explicitly curb the data into a finite length suitable for analysis and processing. This process is called 'Windowing'. In the discussions of the concept of the autocorrelation function (in discrete form) and of the two spectral estimation methods above we implicitly allowed the curbing of the data by multiplying it with a 'Window Function' which in this case is what is called a 'Rectangular Window' given by,

$$w_k = 1; 0 \leq k \leq N-1$$
$$= 0; k < 0,$$

where N is the duration of the data sequence.

The Fourier transform of the rectangular window is given by,

$$F.T\{w_k\} = \frac{Sin(N\omega/2)}{Sin(\omega/2)} e^{-j\omega N/2}$$

Since multiplication in the time domain corresponds to a convolution operation in the frequency domain, the power spectral estimates are no longer exact and accurate but are 'smeared' and hence have reduced frequency resolution. Secondly, the abrupt termination of the data at either of its ends results in the introduction of spurious high frequency estimates (the phenomenon called 'leakage effect'). Also, the spectrum of this window function has several negative excursions and therefore, may cause negative power spectral estimates. To avoid or at least minimise these errors different window functions with gradually tapering ends and non-negative spectral function have been developed, the most popular being the 'Hamming' and the 'Blackman' windows. A review of these is found in Harris [16]. Thus, the data (input data sequence or autocorrelation lags) upon which the above mathematical operations are performed is to be considered multiplied with a window function. The use of window functions help minimise the said errors; however, they also cause reduced frequency resolution because of the convolution operation mentioned above. Therefore, selection of the proper window function is dependent upon the desired application.

## A.2. Modern Methods

During the past two decades, several new spectral estimation procedures have been developed which are particularly attractive for making high resolution spectral estimates when the data record is short. Also they are found useful when one may wish to predict or extrapolate the data or the autocorrelation function. (In the above methods the windowing of the data or the lags makes the implicit assumption that the unobserved data or lag values outside the window are zero, which is normally an unrealistic assumption. Smeared spectral estimates therefore result as a consequence). Perhaps the major advantage these new methods offered was that they provided a mechanism for modelling the data. This can be better explained as follows.

Often one has more knowledge about the process from which the data samples are taken, or at least is able to make a more reasonable assumption other than to assume the data is zero outside a window. Use of *a priori* information (or assumptions) may permit selection of an exact model for the process that generated the data samples, or at least a model that is a good approximation to the actual underlying process. It is then usually possible to obtain a better spectral estimate based on the model by determining the parameters of the model from the observations. Thus spectrum analysis, in the context of modelling, becomes a three step procedure. The first step is to select a time series model for the underlying process. The second step is to estimate the parameters of the assumed model using either the available data samples or autocorrelation lags (either known or estimated from the data). The third step is to obtain the spectral estimate by substituting the estimated model parameters into the theoretical PSD implied by the model. One key feature of this modelling approach to spectral estimation is that only the output process of the model is available for analysis; the input driving process is not assumed available. However, it is promising to know that one can make realistic assumptions concerning the nature of the measured process outside the measurement interval. Thus the need for window functions can be eliminated along with their distorting impact [19]. Based upon such an approach several methods have been developed. However, only a few popular methods are discussed below. Again, a detailed review of these methods is beyond the scope of this discussion and hence, only the relevant theory and mathematical relations are put forth.

### A.2.1. Maximum Entropy Method (MEM)

The MEM power spectral estimation approach can be posed as follows: given (p+1) consecutive estimates of the correlation coefficients of the process $\{x(t)\}$, R(m), m=0,1, . . . ,p, estimate the PSD of the process. Clearly what is needed for the estimation are the unknown correlation coefficients R(m); $m \geq p$. The MEM indeed does that by extrapolating the available autocorrelation coefficients in such a way that the time series characterized by the correlation has maximum entropy (The entropy is a measure of the amount of information we have on a process). Out of all time series having the (p+1) given autocorrelation coefficients, the time series that yields the maximum entropy will be the most random one, or in other words, the estimated PSD will be the flattest among all the PSDs having the given (p+1) coefficients. That is, no new information is added.

The input data is first modelled as a weighted sum of past values plus a noise term, that is,

$$x_n = -\sum_{k=1}^{p} a_k x_{n-k} + e_n$$

The weighting coefficients are called the *autoregression coefficients* of order (in the above case) $p$. Now, the entropy function which is given by,

$$\Delta H = \int_{-\infty}^{\infty} \log_2 P(f)\,df$$

has to be maximised. Since there are an infinite number of signals with white spectrum, the exact input is unknown. However, we know that we want to maximise the entropy (given by the relation above) subject to the constraints that

$$R(m) = \int_{-\infty}^{\infty} P(f) exp(j2\pi f n \Delta t)\,df$$

$$n = 0,1, \ldots, p$$

This constraint maximization will ensure that the estimated spectrum of a process has the flattest spectrum of all the processes with the given p+1 correlation coefficients. Based upon the model assumed above, the power spectral density estimate is then given by,

$$P_{ar}(f) = \frac{\sigma^2 \Delta t}{|1 + \sum_{k=1}^{p} a_k\, exp\,(-j2\pi f k \Delta t)|^2}$$

where, $\Delta$ t is the sampling rate, and $\sigma^2$ is the variance of the input data.

Thus, to estimate the PSD one need only estimate $\{a_1, a_2, \ldots, a_p, \sigma^2\}$.

To do this, a relationship between the autoregressive coefficients and the autocorrelation function (known or estimated) of $x_n$, called the 'Yule-Walker' equations, given below, are used.

$$R(m) = -\sum_{l=1}^{p} a_l R(m-l), m > 0$$

$$= -\sum_{l=1}^{p} a_l R(-l) + \sigma^2, m = 0.$$

Though several algorithms have been developed to solve the above set of equations none of them are discussed here.

### A.2.2. AutoRegressive Moving Average Method (ARMA)

In this method, the data sequence is modelled as the output of a $p$ pole and $q$ zero filter excited by white noise, that is,

$$x_n = -\sum_{k=1}^{p} a_k x_{n-k} + \sum_{k=0}^{q} b_k n_{n-k}$$

where, $n_n$ is the white noise input sequence. The poles of the filter are assumed to be within the unit circle of the $z$-plane while, the zeros may lie anywhere in the plane.

To estimate the above parameters, many techniques involving matrix computations and/or iterative optimization methods have been formulated theoretically. These approaches are not normally practical for real-time processing; thus, suboptimal techniques involving least error squares criterion are widely used. These methods generally estimate the AR (zeros) and the MA (poles) parameters separately rather than jointly as required for optimal parameter estimation [19]. Once the parameters of the ARMA $(p,q)$ model are identified, the spectral estimate is obtained as,

$$P_x(f)=\frac{\sigma^2\Delta t|1+\sum_{k=1}^{q} b_k\,exp\,(-j2\pi fk\Delta t)|^2}{|1+\sum_{k=1}^{p} a_k\,exp\,(-j2\pi fk\Delta t)|^2}$$

where, $\Delta$ t is the sampling rate, and $\sigma^2$ is the variance of the input data.

### A.2.3. Capon's Spectral Estimation Method

This method is based on the idea of measuring the power output of a set of narrow band (optimal) filters. We have seen that the effect of unavoidable windowing of the data is to distort the power spectral estimation. The sidelobes of the window cause 'leakage' from neighbouring frequencies into the estimate of the frequency of interest. Suppose, however, that for each frequency of interest, we filter the data by means of an optimal filter in such a way that contribution from other frequencies be minimised. This can be viewed as a set of narrow bandpass filters, each optimally designed for the particular frequency. The power spectrum is then estimated by calculating the power output of these filters.

Given a data sequence $\{x_k\}$, to estimate its power spectrum the data is filtered with a Moving Average (MA) filter with coefficients to be optimally adjusted. Ideally, we are interested in the output power of an infinitly narrow bandpass filter at the frequency $\omega$. The MA filter predicts the $k^{th}$ value of the output in the following manner,

$$x_k=\sum_{n=0}^{N-1} b_n x_{k-n}$$

In order to achieve the 'narrowness' through the above filter, we have to find the optimal value of the filter coefficients $b_n$, n =0,1, . . . , N-1, such that the variance of $x_k$ is minimal. In other words, we consider the input to the above filter (the observed sequence) as given by

$$x_k = A\,exp(jwk\Delta t) + n_k$$

where $\{n_k\}$ is the noise sequence appearing due to the leakage (also the variance of the estimate as mentioned above) and A is the amplitude of the sinusoid component whose power spectral density is to be estimated.

In proceeding further, we obtain the variance of the output as,

$$\sigma^2 = B^H R_{xx} B$$

where B is the transpose of the matrix of coefficients $(b_k)$,
H is the complex conjugate transpose, and
$R_{xx}$ is the autocorrelation matrix of $x_k$

and to minimise the above, also a constraint given as

$$E^H A = 1$$

where, E is the vector

$$E = [1, exp(j2\pi f_0 \Delta t), \cdot \cdot \cdot, exp(j2\pi [p-1] f_0 \Delta t)]^T$$

The solution to the filter coefficients can be shown to be

$$B_{opt} = \frac{R_{xx}^{-1} E}{E^H R_{xx}^{-1} E}$$

and the minimum output variance to be

$$\sigma^2{}_{min} = \frac{1}{E^H R_{xx}^{-1} E}.$$

Since the minimum output variance is due to frequency components near $f_0$ (the frequency response at which is seen to be unity), then $\sigma^2{}_{min} \Delta\ t$ can be interpreted as a power spectral estimate. Thus, the Capon's spectral estimate is defined as

$$P_{CE}(f_0)=\frac{\Delta t}{E^H R_{xx}^{-1} E}.$$

To compute the spectral estimates, therefore, one only needs an estimate of the autocorrelation matrix.

## A.3. Comparisons between the Traditional and Modern Methods

All the three modern methods detailed above are very suitable for short data records. Their efficacy in both obtaining high resolution and less estimation errors stands out compared to the traditional methods only in short data records [19]. Of course, they also serve as an efficient way of modelling the process generating the data observed unlike the traditional methods.

But computationally, the traditional approaches are more efficient than the modern methods. Having *a priori* information of the process would however help speed up the latter. In both the Blackman-Tukey and the Welch's methods, the variance of the estimates obtained by them can be computed, while there has been no consistent way of determining the same in any of the modern methods [8]. For short data records, the resolution obtained by the three modern methods have been found better than the Blackman-Tukey approach.

Since the best choice of the model order in any of the three modern methods is not generally known *a priori*, it is usually necessary in practice to postulate several model orders. Based on these, one then computes some error criterion that indicates which model order to choose. Too low a guess for model order results in a highly smoothed spectral estimate. Too high an order introduces spurious detail into the spectrum. Some criteria (like the Akaike Criterion) have been developed to select the optimal order.

On the whole, the practice of spectral estimation, both traditional and modern, has more of an empirical basis and less of a solid theoretical basis. With finite data records as is the case in general, spectral estimation is not an exact science and in fact, a great deal of experimentation and subjective trade-off is usually required.

## A.4. Definitions of some Spectral Parameters

To characterise a power spectrum, several parameters have been consistently used in the study of myoelectric signals. They are all defined below:

**Mean Power Frequency**

It is that frequency, $f_{mean}$ which is given by,

$$f_{mean} = \frac{\int_0^{\infty} f \times P(f)\,df}{\int_0^{\infty} P(f)\,df}$$

**Median Frequency**

It is the frequency, $f_{med}$ which divides the power spectrum into two power halves. That is,

$$\int_0^{f_{med}} P(f)\,df = \int_{f_{med}}^{\infty} P(f)\,df = \frac{1}{2}\int_0^{\infty} P(f)\,df$$

**Peak Power Frequency**

The peak power frequency, $f_{peak}$ is the frequency which assumes the maximum power value in the power spectrum.

**Spectral Ratios**

These are ratios of power in several arbitrarily chosen bands, in the power spectrum, of equal or unequal widths used to monitor spectral power shifts from one set of frequencies to another.

**Spectral Bandwidth**

It is that frequency range in the power spectrum which suffers no more than 3 dB attenuation. The 3 dB points mark the values of power equal to half of the maximum obtained.

**Spectral Power**

It is the area beneath the power spectral curve. Mathematically,

$$\text{Spectral Power} = \int_0^{\infty} P(f)\,df$$

# Appendix B
# SPECTRAL ESTIMATION PROCEDURES

The following two command procedures (with comments) are provided for computing the power spectra using the Blackman-Tukey and the Welch's methods. They are to be executed in the Interactive Laboratory System's (ILS) domain on a VAX 11/780. Both the procedures require a ILS data file containing the sampled data divided into segments the number of which, is an user's choice for each of the estimation schemes. Also a digital bandpass filter (5-450 Hz) has to be synthesised using the ILS and stored in the 'common file' (CM9999.).

**Blackman-Tukey's Spectral Estimation**

```
$ FIL SNIP'P1'
$ OPN S            * Conversion into ILS records *
$ SRE 1,'P3'
$ FIL NIP'P1'
$ FIL SNFIP'P1'
$ OPN S            * Bandpass Filtering (5-450 Hz) *
$ FLT R
$ FIL NFIP'P1'
$ FIL SNCORR'P1'
$ OPN S            * Autocorrelation computation *
$ COR A1,1
$ FIL NCORR'P1'
$ FIL SNFFT'P1'
$ OPN S            * Fast Fourier Transformation *
$ FFT F,,,3,
$ FIL NFFT'P1'
$ FIL SNPOW'P1'
$ OPN S
$ UOP MA1,1        * Scaling performed *
$ FIL NPOW'P1'
```

```
$ DRE M            * Display Power Spectrum *
$ EXIT
```

**Welch's Spectral Estimation**

```
$ FIL SNIP'P1'
$ OPN S            * Conversion into ILS records *
$ SRE 1,'P3'
$ FIL NIP'P1'
$ FIL SNFIP'P1'
$ OPN S            * Bandpass Filtering (5-450 Hz) *
$ FLT R
$ FIL NFIP'P1'
$ FIL SNFFT'P1'
$ OPN S            * Fast Fourier Transformation *
$ FFT F,,,3,
$ FIL NFFT'P1'
$ FIL SNABFF'P1'
$ OPN S
$ UOP AB1,'P3'
$ COPY ABFF'P1' ABFF'P2'    * Squaring absolute values *
$ FIL NABFF'P1'
$ FIL BNABFF'P2'
$ FIL SNTPOW'P1'
$ OPN S            * Segmental Power Spectra computed *
$ BOP M
$ FIL NTPOW'P1'
$ FIL SNFPOW'P1'
$ OPN S
$ AVG 01,20        * Average Power Spectrum computed *
$ FIL NFPOW'P1'
$ FIL SNPOW'P1'
$ OPN S
$ UOP MA1,1        * Scaling performed *
$ FIL NPOW'P1'
$ DRE M            * Display Power Spectrum *
$ EXIT
```

# Appendix C
# TABULATED RAW DATA

In this appendix are recorded the raw data obtained from the two studies comprising the work detailed in this thesis. The data have been tabulated in the following manner. The Tables C-1 to C-4 pertain to the data namely, the median frequencies and the spectral powers as obtained for the five different subjects in the first study. The first study comprising two cases involved the study of variation in joint angle (and hence muscle length) causing any spectral changes as could be monitored by the above two parameters. Tables C-5 to C-14 contain the results of the second study namely, that studying the spectral changes caused by varying the applied torque and the angular velocity of contraction. Table C-15 gives the stepwise multiple regression equation estimates, as obtained for one of the subjects, from the equation given in chapter four. The median frequency is given in terms of Hertz and the spectral power in Watts.

| S \ JA | 165 | 150 | 135 | 120 | 105 | 90 | 75 | 60 |
|---|---|---|---|---|---|---|---|---|
| 1 | 61 | 72.5 | 76.5 | 88 | 94.5 | 71 | 64 | 72 |
| 2 | 67.5 | 68.5 | 69 | 72 | 76 | 75 | 74 | 68.5 |
| 3 | 58.5 | 63.5 | 78 | 97 | 103 | 71 | 78.5 | 73 |
| 4 | 49.8 | 55 | 60.5 | 69 | 79 | 74.5 | 74 | 68 |
| 5 | 60.5 | 61.5 | 70.5 | 78.5 | 90 | 108.5 | 97 | 75.5 |

**Table C-1**: Median Frequencies obtained for different Joint Angles for a load 19.6 N (study 1)

| S \ JA | 165 | 150 | 135 | 120 | 105 | 90 | 75 | 60 |
|---|---|---|---|---|---|---|---|---|
| 1 | 2.2 | 1.6 | 1.8 | 1.8 | 1.2 | 0.4 | 0.7 | 1.4 |
| 2 | 2.3 | 1.6 | 0.9 | 0.6 | 0.3 | 0.2 | 0.24 | 0.41 |
| 3 | 1.3 | 1.1 | 1.5 | 0.99 | 0.58 | 0.41 | 0.99 | 2.2 |
| 4 | 2.5 | 1.9 | 0.99 | 0.76 | 0.5 | 0.3 | 0.27 | 0.4 |
| 5 | 1.8 | 1.6 | 1.8 | 1.3 | 0.9 | 0.2 | 0.3 | 0.5 |

**Table C-2**: Spectral Powers obtained for the same

| S \ JA | 150 | 90 | 60 |
|---|---|---|---|
| 1 | 44 | 95 | 106 |
| 2 | 96 | 149 | 115 |
| 3 | 89 | 109 | 109 |
| 4 | 66 | 140 | 97 |
| 5 | 62 | 97 | 87 |

**Table C-3:** Median Frequencies obtained for different Joint Angles for a load of 29.4 N (study 1)

| S \ JA | 150 | 90 | 60 |
|---|---|---|---|
| 1 | 1.34 | 0.51 | 0.49 |
| 2 | 0.64 | 0.44 | 0.54 |
| 3 | 0.58 | 0.53 | 0.64 |
| 4 | 0.81 | 0.36 | 0.61 |
| 5 | 1.2 | 0.44 | 0.33 |

**Table C-4:** Spectral Powers obtained for the same

| T \ V | 40 | 80 | 120 | 160 |
|---|---|---|---|---|
| 1.23 | 54.6 | 43 | 59 | 53 |
| 2.45 | 56 | 50 | 63 | 58 |
| 3.68 | 64 | 60.5 | 65 | 63 |
| 7.35 | 73 | 75 | 68.5 | 72 |

**Table C-5:** Median Frequencies obtained for different Torque-Velocity combinations for subject no.1

| T \ V | 40 | 80 | 120 | 160 |
|---|---|---|---|---|
| 1.23 | 0.13 | 0.16 | 0.18 | 0.4 |
| 2.45 | 0.2 | 0.3 | 0.85 | 0.87 |
| 3.68 | 0.36 | 0.44 | 0.81 | 1.0 |
| 7.35 | 0.7 | 0.88 | 2.1 | 2.2 |

**Table C-6:** Spectral Powers obtained for the same

| T \ V | 40 | 80 | 120 | 160 |
|---|---|---|---|---|
| 1.23 | 61 | 36 | 55 | 51 |
| 2.45 | 63 | 65 | 60 | 57 |
| 3.68 | 63 | 70 | 66 | 64 |
| 7.35 | 73 | 77 | 66 | 80 |

**Table C-7:** Median Frequencies obtained for different Torque-Velocity combinations for subject no.2

| T \ V | 40 | 80 | 120 | 160 |
|---|---|---|---|---|
| 1.23 | 0.04 | 0.08 | 0.2 | 0.12 |
| 2.45 | 0.06 | 0.08 | 0.38 | 0.59 |
| 3.68 | 0.12 | 0.24 | 0.63 | 0.77 |
| 7.35 | 0.39 | 0.42 | 1.6 | 2.2 |

**Table C-8:** Spectral Powers obtained for the same

| T \ V | 40 | 80 | 120 | 160 |
|---|---|---|---|---|
| 1.23 | 72 | 81 | 80 | 76 |
| 2.45 | 83 | 88 | 80 | 86 |
| 3.68 | 91 | 91 | 94 | 94 |
| 7.35 | 91 | 96 | 96 | 98 |

**Table C-9:** Median Frequencies obtained for different Torque-Velocity combinations for subject no.3

| T \ V | 40 | 80 | 120 | 160 |
|---|---|---|---|---|
| 1.23 | 0.06 | 0.17 | 0.2 | 0.32 |
| 2.45 | 0.1 | 0.5 | 0.68 | 0.80 |
| 3.68 | 0.17 | 0.19 | 0.41 | 0.8 |
| 7.35 | 0.37 | 0.46 | 1.1 | 1.8 |

**Table C-10:** Spectral Powers obtained for the same

| T \ V | 40 | 80 | 120 | 160 |
|---|---|---|---|---|
| 1.23 | 71 | 58 | 65 | 57 |
| 2.45 | 77 | 70 | 68 | 63 |
| 3.68 | 77 | 73 | 74 | 65 |
| 7.35 | 78 | 78 | 78 | 72 |

**Table C-11:** Median Frequencies obtained for different Torque-Velocity combinations for subject no.4

| T \ V | 40 | 80 | 120 | 160 |
|---|---|---|---|---|
| 1.23 | 0.09 | 0.11 | 0.19 | 0.36 |
| 2.45 | 0.1 | 0.3 | 0.62 | 0.64 |
| 3.68 | 0.16 | 0.27 | 0.56 | 1.55 |
| 7.35 | 0.39 | 0.41 | 1.59 | 2.2 |

**Table C-12:** Spectral Powers obtained for the same

| T \ V | 40 | 80 | 120 | 160 |
|---|---|---|---|---|
| 1.23 | 73 | 76 | 70 | 62 |
| 2.45 | 77 | 79 | 71 | 70 |
| 3.68 | 77 | 85 | 73 | 72 |
| 7.35 | 89 | 85 | 84 | 82 |

**Table C-13:** Median Frequencies obtained for different Torque-Velocity combinations for subject no.5

| T \ V | 40 | 80 | 120 | 160 |
|---|---|---|---|---|
| 1.23 | 0.05 | 0.14 | 0.31 | 0.24 |
| 2.45 | 0.08 | 0.29 | 0.63 | 0.79 |
| 3.68 | 0.2 | 0.3 | 0.8 | 1.05 |
| 7.35 | 0.55 | 0.95 | 1.54 | 2.47 |

**Table C-14:** Spectral Powers obtained for the same

| T \ V | 40 | 80 | 120 | 160 |
|---|---|---|---|---|
| 1.23 | 52.05 | 50.58 | 49.12 | 47.65 |
| 2.45 | 55.66 | 54.20 | 52.73 | 51.27 |
| 3.68 | 59.31 | 57.84 | 56.38 | 54.91 |
| 7.35 | 70.18 | 68.72 | 67.25 | 65.79 |

**Table C-15:** Regression equation estimates of one subject